Supporting Information For

Selectively Lighting Up Two-Photon Photodynamic Activity in Mitochondria with AIE-Active Cyclometalated Iridium(III) Complexes

Jiangping Liu, ‡[a] Chengzhi Jin, ‡[a] Bo Yuan,[a] Xingguo Liu,[b] Yu Chen,[a] Liangnian Ji,[a] and Hui Chao*[a]

[a] MOE Key Laboratory of Bioinorganic and Synthetic Chemistry, School of Chemistry, Sun Yat-Sen University, Guangzhou 510275, China. E-mail: ceschh@mail.sysu.edu.cn, Fax: 86-20-84112245, Tel: 86-20-84110613

[b] Guangzhou Institute of Biomedicine and Health, Chinese Academy of Sciences, Guangzhou, 510530, China

Content

Materials

Unless otherwise noted, all chemical reagents and solvents were commercially available and used without further purification. Twice-distilled water was used throughout all of the experiments. $IrCl_3 \cdot xH_2O$, cisplatin, 2-(2,4-difluorophenyl)pyridine (dfppy), 3-(4,5-dimethylthiazol-2-yl)-2,5-diphenyltetrazolium bromide (MTT), Ir standard solution (1000 μg/mL), 1,3-diphenyliso-benzofuran (DPBF), PBS , sodium pyruvate, rhodamine B and 2',7'-dichlorofluorescin diacetate (DCF-DA) were purchased from Sigma-Aldrich (USA). Annexin V-FITC/propidium iodide apoptosis detection kit was purchased from Life Technologies. MitoTracker Green was obtained from Invitrogen. Caspase-3/7 activity kit, CellTiter-Glo® 3D Cell Viability kit and CellTiter-Glo® Luminescent Cell Viability kit were purchased from Promega (USA). XF Cell Mito Stress Test Kit and XF Glycolysis Stress Test Kit were bought from Seahorse Bioscience Agilent. Nucleus extraction kit and cytoplasm extraction kit were purchased from Thermo pierce.

Instruments

Microananlysis (C, H and N) was performed using a Perkin-Elmer 240Q elemental analyzer. Electrospray ionization mass spectra (ES-MS) were recorded on a LCQ system (Finnigan MAT, USA). The ^1H NMR and ^{13}C NMR spectra were recorded on a Bruker BioSpin AVANCE III 400MHz Nuclear Magnetic Resonance Spectrometer. The UV-Vis spectra were recorded on a Varian Cary 300 spectrophotometer. Emission spectra were recorded on a PerkinElmer LS 55 fluorescence spectrometer at room temperature. Two-photon absorption cross section measurements were performed by a modelocked Ti: Sapphire laser (Coherent, USA) with a repetition rate of 80 MHz, and a femtosecond optical parametric amplifier (spectral tuning range 720–850 nm). Luminescence lifetime studies were performed with an Edinburgh FLSP-920 photo-counting system using a pulse laser (405 nm) as the excitation source. Luminescence quantum yields of iridium complexes in an aerated DMSO-H_2O binary solution were measured with reference to $[Ru(bpy)_3]^{2+}$ (Φ_{PL} = 0.040, aerated water, 25 ˚C)[1] by a reported method.[2] The inductively coupled plasma mass spectrometry (ICP-MS) experiments were carried out on an Agilent's 7700x instrument. Cell imaging was conducted on a LSM 710 (Carl Zeiss, Germany) Laser Scanning Confocal Microscope. Visible one-photon irradiation (λirr = 405 nm, 40 mW/cm^2) in PDT was provided by a commercially available LED visible area light source (Height LED Instruments, China). OCR and ECAR were determined by a Seahorse XF-24 extracellular flux analyzer (Seahorse Bioscience). All data were processed with the OriginPro 8.0 software package. HPLC was conducted by Aligent 1260 Infinity High Performance Liquid Chromatograph with Inertsil ODS-3 as chromatographic column.

Synthesis and characterization

1,10-Phenanthroline-5,6-dione,[3] 2-phenylbenzo[d]thiazole (**pbt**),[4] dibenzo[f,h]quinoxaline (**dbq**),[5] $[Ir(dfppy)_2Cl]_2$,[5] $[Ir(bpt)_2Cl]_2$,[4] $[Ir(dbq)_2Cl]_2$[5] were prepared according to previously published method. The main ligand, N,N-diphenyl-4-(1-phenyl-1H-imidazo[4,5-f][1,10]phenanthrolin-2-yl)aniline (**dpipa**), was synthesized and purified as described in our previous work.[6] **Ir1-Ir3** synthetic routes were depicted in Scheme S1.

General synthetic procedure of Ir1-Ir3: A mixture of **dpipa** (0.2 mmol) and the corresponding chloro-bridged iridium dimer complex (0.1 mmol) in $CHCl_3/CH_3OH$ (30mL/15mL) was refluxed and protected from

light under

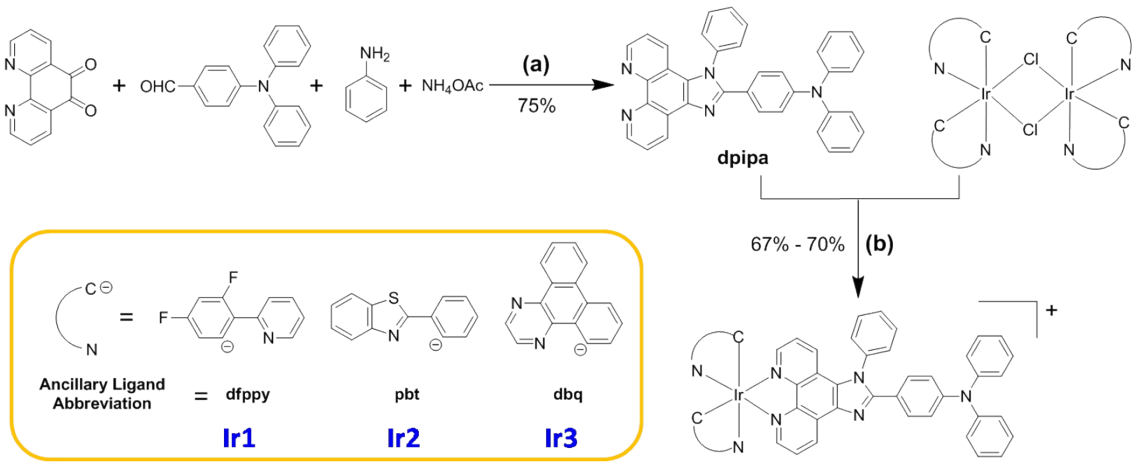

Scheme S1. Synthetic routes of **Ir1-Ir3**. (a) CH_3COOH, reflux overnight.[6] (b) $CHCl_3/CH_3OH$ (2:1, v/v), Ar, 65 °C, ,dark, 12 h.

an argon atmosphere at 65 °C for 12 hours. Upon completion, the solution was evaporated to dryness. The resultant solid was purified by column chromatography on alumina with CH_3CN/EtOH to afford the pure product. The yield, ES-MS, ^{1}H NMR, and elemental analysis data are listed below.

Ir1: Yield 145.5 mg, 70.2%. Anal. Calcd. for $C_{59}H_{37}N_7F_4ClIr$ (%): C, 61.75; H, 3.25; N, 8.54. Found (%): C, 61.43; H, 3.67; N, 8.49. ^{1}H NMR (400 MHz, d_6-DMSO) δ 9.33 (dd, J = 8.3, 1.4 Hz, 1H), 8.30 (dt, J = 12.8, 7.6 Hz, 3H), 8.21 – 8.09 (m, 2H), 8.07 – 7.91 (m, 2H), 7.84 – 7.67 (m, 6H), 7.56 (d, J = 6.0 Hz, 2H), 7.54 – 7.45 (m, 3H), 7.42 – 7.29 (m, 4H), 7.15 (dd, J = 10.6, 4.2 Hz, 2H), 7.13 – 7.04 (m, 6H), 7.07 – 6.92 (m, 2H), 6.92 – 6.77 (m, 2H), 5.70 (ddd, J = 13.2, 8.3, 2.3 Hz, 2H). ^{13}C NMR (100 MHz, d_6-DMSO) δ 165.42, 164.38, 163.28, 162.24, 160.22, 160.12, 155.12, 154.69, 154.10, 150.30, 150.20, 149.31, 149.16, 146.63, 144.50, 144.32, 140.46, 137.28, 136.21, 133.44, 131.70, 131.46, 130.61, 130.32, 129.24, 128.18, 127.28, 126.42, 126.86, 124.94, 123.92, 123.76, 122.51, 121.68, 120.43, 113.91, 113.78, 99.64. ES-MS (CH_3OH): m/z = 1001.20 $[M-Cl]^+$.

Ir2: Yield 156.5 mg, 68.3%. Anal. Calcd. for $C_{63}H_{41}N_7S_2ClIr$ (%): C, 63.70; H, 3.48; N, 8.25. Found (%): C, 63.52; H, 3.71; N, 8.16. ^{1}H NMR (400 MHz, DMSO) δ 9.34 (dd, J = 8.3, 1.4 Hz, 1H), 8.44 (dd, J = 5.1, 1.4 Hz, 1H), 8.31 – 8.13 (m, 4H), 8.05 (dd, J = 11.7, 7.4 Hz, 2H), 7.96 – 7.82 (m, 2H), 7.76 (td, J = 5.3, 2.2 Hz, 3H), 7.72 – 7.62 (m, 1H), 7.53 (dd, J = 8.7, 1.1 Hz, 1H), 7.49 – 7.41 (m, 2H), 7.34 (ddd, J = 20.5, 10.3, 4.7 Hz, 6H), 7.22 – 7.11 (m, 4H), 7.10 (ddd, J = 22.3, 12.6, 8.3 Hz, 6H), 6.98 (tdd, J = 14.0, 6.4, 1.2 Hz, 4H), 6.89 – 6.73 (m, 2H), 6.37 (dd, J = 7.5, 2.0 Hz, 2H), 5.86 (d, J = 8.4 Hz, 1H), 5.80 (d, J = 8.4 Hz, 1H). ^{13}C NMR (100 MHz, d_6-DMSO) δ 181.26, 181.21, 153.83, 150.43, 149.91, 149.65, 148.67, 148.53, 146.00, 144.82, 144.69, 140.05, 136.66, 135.75, 132.88, 132,68, 132.60, 132.05, 132.00, 130.79, 129.96, 129.74, 128.84, 128.05, 127.98, 127.33, 126.64, 125.75, 125.37, 125.02, 124.40, 123.14, 120.98, 119.67, 119.55, 116.41. ES-MS (CH_3OH): m/z = 1110.15 $[M-Cl]^+$.

Ir3: Yield 170.5 mg, 67.2%. Anal. Calcd. for $C_{69}H_{43}N_9ClIr$ (%): C, 67.61; H, 3.54; N, 10.28. Found (%): C, 67.56; H, 3.76; N, 10.21. ^{1}H NMR (400 MHz, DMSO-d6) δ 9.32 (dd, J = 8.4, 1.5 Hz, 1H), 9.15 (td, J = 8.0, 1.4 Hz, 2H), 8.84 (dd, J = 13.3, 8.3 Hz, 2H), 8.73 (t, J = 3.3 Hz, 2H), 8.37 (dd, J = 15.2, 8.2 Hz, 2H), 8.27 (dd, J = 5.2, 1.5 Hz, 1H), 8.14 – 8.04 (m, 4H), 7.95 (dddd, J = 9.6, 8.4, 7.2, 1.5 Hz, 2H), 7.92 – 7.84 (m, 2H), 7.84 –

7.72 (m, 4H), 7.68 (dd, J = 8.7, 5.1 Hz, 1H), 7.55 – 7.49 (m, 2H), 7.45 (dd, J = 8.7, 1.4 Hz, 1H), 7.39 – 7.32 (m, 7H), 7.14 (tt, J = 7.4, 1.2 Hz, 2H), 7.11 – 7.05 (m, 5H), 6.91 – 6.79 (m, 2H), 6.57 (d, J = 7.3 Hz, 1H), 6.53 (d, J = 7.3 Hz, 1H). ^{13}C NMR (100 MHz, d_6-DMSO) δ 223.02, 220.73, 218.34, 217.71, 215.66, 215.11, 214.23, 214.02, 212.58, 211.84, 207.15, 206.36, 205.80, 202.38, 201.91, 201.52, 200.93, 200.52, 199.62, 199.34, 198.95, 198.24, 198.00, 197.80, 197.17, 195.45, 194.86, 193.95, 191.48, 190.75, 189.52, 186.14 ES-MS (CH_3OH): m/z = 1189.80 $[M-Cl]^+$.

Crystallographic structure determination

Crystals of main ligand **dpipa** and complex **Ir1** suitable for X-ray analysis were obtained by slowly evaporating the chloroform-toluene solvents at room temperature. X-ray diffraction measurements were carried out on an Oxford Xcalibur Nova diffractometer equipped with Cu Kα radiation (**Ir1**) (λ = 1.54184 Å) and a Bruker SMART diffractometer equipped with Mo Kα radiation (**dpipa**) (λ = 0.71073 Å). An absorption correction was applied by an empirical absorption correction (**Ir1**)[7] SHELXS-2014 program incorporated in the OLEX2 program package was employed to directly solve the compound structure and full-matrix least-squares refinement based on F^2.[8] All of the hydrogen atoms were included in the calculated positions and refined with isotropic thermal parameters riding on the positions of the parent atoms. In the structure of Ir1, the disorders of the complex Ir1 emerged in both one of the ancillary ligands (2f-ppy) and the triphenylamine moiety of the main ligand (dpipa). In refinement, these disorders were handled by the using "PART" instruction in the SHELXL-2014 software.[8b] The disordered solvent molecules were removed utilizing the SQUEEZE routine in the PLATON software.[9] The crystal data and structural refinements are shown in Table S1, S3. And the selected bond length and angles are listed in Table S2, S4. CCDC 1503268 (**dpipa**) and 1503269 (**Ir1**) contain the supplementary crystallographic data for this paper; these data can be obtained at http://www.ccdc.cam.ac.uk/.

Singlet oxygen detection in solution

Both direct and indirect methods were employed to detect singlet oxygen generated by the indicated complexes in various solvent ratio of DMSO aqueous solution. The direct verification of singlet oxygen generation is to detect the singlet oxygen phosphorescence generated from the activated indicated compounds solution at 1270 nm under irradiation (λ_{irr} = 405 nm).[10] For indirect method, DPBF of which the luminescence intensity decreases after scavenging singlet oxygen was used to reflect the singlet oxygen level generated by the indicated compounds under irradiation (405 ± 10 nm, 40 mW cm^{-2}, 1 second per spot). The decomposition of DPBF was monitored by the emission decline at 479 nm. The concentration of compounds were adjusted to OD_{405nm} = 0.25 in both sections.

Two-photon absorption cross sections determination[11]

The two-photon absorption cross sections determination was performed acoording to a matured theoretical framwork and experimental protocol developed by Webb and Xu[12]. The two-photon induced luminescence of the iridium complexes was measured through quartz cuvettes in 10% content of DMSO aqueous solution. The samples were exited with laser pulses of 100 fs produced by the mode-locked Ti:Sapphire laser with a repetition rate of 80 MHz, and a femtosecond optical parametric amplifier was utilized. The emission from

the aqueous suspensions was collected at a 90 degree angle by high numerical aperture lens and directed to a spectrometer's entrance slit. Rodamine B was utilized as the reference. The quadratic dependence of the two-photon induced luminescence intensity on the exitation power was verified at the cooresponding wavelength of their respective maximal two-photon absorption cross sections. The two-photon exitation raitios of the reference and sample can be expressed as the following formula,

$$\sigma_S = \sigma_R \frac{\phi_R C_R I_S n_S}{\phi_S C_S I_R n_R}$$

in which σ represents the TPA cross sections, Φ stands for the quantum yield, C is the concentration, I is the integrated luminescence intensity and n is the refractive index. Subscript "S" stands for sample and "R" stands for reference, i.e. Rodamine B.

Partition-coefficient (Log *P*) measurement

The partition-coefficient of each complex, expressed as[13]

$$\log P^0_{o/w} = \log\left(\frac{[solute]_{octanol}}{[solute]_{water}}\right)$$

can be determined by "shake-flask" method. Water and octanol were mixed and fully shaken to equilibrant and the resultant two layers were separated. The indicated complexes were dissolved in the octanol phase which was previously saturated with water to give a 3 mL solution. The same volume of water phase previously saturated with octanol was added into the solution. The mixture was shaken vigorously at room temperature for 1 hour. The concentration of **Ir1-Ir3** was determined by UV-vis spectroscopy using extinction coefficients of the complexes in octanol saturated with water. The evaluation was replicated for three times.

Cell culture

HeLa/L02 cells were obtained from the American Type Culture Collection (ATCC, Manassas, VA). The cell lines were maintained in DMEM media supplemented with fetal bovine serum (10%), penicillin (100 units/mL) and streptomycin (50 units/mL) at 37 °C in a CO_2 incubator (95% relative humidity, 5% CO_2).

Time dependent ICP-MS

HeLa/L02 cells (*ca.* 1.5 × 10^6 cells) were incubated with 0.5 μM **Ir1** complexes (0.5% DMSO, v%) for varying durations of time (4, 8, 16, 20, 30, 60 min). After washing with PBS for three times and trypsinization, the cells were harvested, centrifuged and resuspended, the cell numbers were subsequently accurately counted. Then all samples were digested by 60% nitric acid at room temperature for at least 24 h. Each sample was then diluted with twice-distilled water to obtain 2% HNO_3 sample solutions. In addition, a standard curve was made for the quantitative determination by use of Ir standard solution (1000 μg/mL). The samples and standard solution were subjected to ICP-MS. The average Ir content in each cell was determined by ICP-MS associated with the total cell numbers.

Intracellular localization studies

The intracellular localization studies are consist of co-staining confocal microscopy and ICP-MS study. Firstly,

in co-localizaiton confocal microscopy, HeLa cells were seeded onto 35 mm confocal dishes (Corning) at a density of 1 × 10^4 cells/mL and allowed to adhere overnight. Prior to incubation with 50 nM MitoTracker Green for 30 min, the cells were loaded with 0.5 μM **Ir1**-**Ir3** complexes (0.5% DMSO, v%) for 30 min at 37 °C, respectively. Confocal images were aquired after the cells were washed with PBS.

In ICP-MS experiment, HeLa cells (*ca.* 1.5 × 10^6 cells) were incubated with 0.5 μM **Ir1**-**Ir3** complexes (0.5% DMSO, v%) for 30 min at 37 °C, respectively. After washing, trypsinization and counting, HeLa cells were equally divided into two parts for the determination of iridium content in nuclei and cytoplasm. One part was proceeded acoording to the protocol of nucleus extration kit while the other one acoording to the protocol of cytoplasm extraction kit. Both extratants were digested by 60% nitric acid at room temperature for at least 24 h. And subsequently processed by the aforementioned method.

Cellular entry mechanism studies

Cellular imaging was launched to study the uptake mechanism.[14] HeLa cells were seeded on 35 mm confocal dishes (Corning) at a density of 1 × 10^4 cells/mL and allowed to adhere overnight. The culture medium were refreshed with PBS. For temperature dependent uptake study, HeLa cells were directly incubated with 0.5 μM **Ir1** complexes (0.5% DMSO, v%) for 30 min at 37 °C or 4 °C. For biol inhibitor dependent study, 2-deoxy-D-glucose (50 mM) and oligomycin (5 μM) were adopted as the metabolic inhibitors and NH_4Cl (50 mM) and chloroquine (100 μM) were used as the endocytic inhibitors. HeLa cells were pretreated with various biol inhibitors for 1 h at 37 °C, respectively, PBS was used to wash the cells upon completion and the cells were further incubated solely with 0.5 μM **Ir1** complexes (0.5% DMSO, v%) for 30 min at 37 °C. All of the cells were finally washed with PBS for three times and subjected to confocal microscopy.

Intracellular co-localization monitoring by CLSM

HeLa cells were seeded onto 35 mm confocal dishes (Corning) at a density of 1 × 10^4 cells/mL and allowed to adhere overnight. Following the co-incubation with 50 nM MitoTracker Green and 50 nM LysoTracker Red for 45 min at 37 °C, the cells were then washed with PBS, exposed to culture medium containing 0.5 μM **Ir1** (0.5% DMSO, v%) in the ambient of real-time culture apparatus equiped by CLSM for 20 min and kept from light. Confocal images were aquired every 4 min during this period. For the MitoTracker Green channel, the excitation wavelength is 488 nm, the signals were collected between 505-525 nm. For the LysoTracker Red channel, the probe was excited at 543 nm, and the emission filter was between 590-650 nm. For the **Ir1** channel, the excitation wavelength was 405 nm, and the emission filter was between 550-585 nm.

HeLa cell metabolism test

The measurement of oxygen consumption rate (OCR) and extracellular acidification rate (ECAR) were performed in real time with a Seahorse XF-24 extracellular flux analyzer according to the protocols of the manufaturer. HeLa cells at a concentration of 5 × 10^4 cells/well were used for measurement. The day before test, the sensor catridge was immersed in calibration buffer and incubated at 37 °C in non-CO_2 incubator overnight. The OCR assay medium was prepared with sodium pyruvate (2 mM), glucose (25 mM and L-

glutamine (2 mM) and ECAR assay medium was prepared with L-glutamine (4 mM). The prepared culture medium was adjusted to pH 7.4, sterilized and stored at 4 °C. HeLa cells were incubated with 0.5 μM **Ir1-Ir3** complexes (0.5% DMSO, v%) for 1 h in the dark. For the light group, the cells were subsequently exposed to LED area light source (405 ± 10 nm, 40 mW cm^{-2}, light dose = 12 J cm^{-2}) while the dark group stay in the dark. Both groups were incubated for additional 1 h and the cell metabolism were assessed including OCR and ECAR which were measured sequentially before and after the addition of injection reagents: oligomycin A as the ATP coupler (0.5 μM), p-trifluoremethoxyphenylhydrazone (FCCP) as the ETC accelerator (500 nM), antimycin A as a complex III inhibitor (0.5 μM) and rotenone as a complex I inhibitor (0.5 μM). OCR and ECAR levels were recorded by the sensor cartridge and the measured values were calibrated based on the cell viability tested in viability assay. As for measurement of glycolytic parameters, the ECAR values were recorded in response to a sequential addition of D-glucose to assess glycolysis, oligomycin to measure maximal glycolytic capacity, and 2-deoxy-D-glucose (2-dG) to measure glycolytic reserve. As for measurement of OXPHOS parameters, the OCR values were recorded in response to another sequential injections of oligomycin A to teminate basal respiration, FCCP to measure ETC accelerator response, and a combination of rotenone and antimycin A to measure non-mitochondrial respiration.

Caspase-3/7 activation detection

Caspase-3/7 activity was measured using Capspase-Glo® Assay kit (Promega) following the protocol of the manufacturer. HeLa cells cultured in white-walled non-transparent 96-well microplates (1.5 × 10^4 cells/well) were incubated with 0.5 μM **Ir1-Ir3** complexes (0.5% DMSO, v%) for 12 h in the dark. The negative control was incubated with solely culture medium, and vehicle-treated cells were also tested in this experiment. Cisplatin was adopted as the positive control. For the light group, the plates were exposed to LED area light irradiation (405 ± 10 nm, 40 mW cm^{-2}, light dose = 12 J cm^{-2}); for the dark group, the plates were kept in the dark. The incubation proceeded for additional 2 h in the dark for all plates. Upon completion, 100 μL of Caspase-Glo® 3/7 reagent was added to each well which contained 100 μL culture medium. The incubation proceeded for 1 h at room temperature and protected from light. The luminescence intensity was measured by a multifunction microplate reader (infinite M200 PRO, TECAN).

Detection of two-photon induced intracellular singlet oxygen

HeLa cells were seeded on confocal dishes (Corning) at a density of 1 × 10^4 cells/mL and allowed to adhere overnight. The cells preincubated with 0.5 μM **Ir1-Ir3** (0.5% DMSO, v%) for 30 min at 37 °C, respectively were futher incubated with 2 mL PBS containing 10 μM DCFH-DA[15] for 20 min. The culture medium was refreshed with fresh PBS after this period and sbujected to two-photon irradiation for 50 s (0.88 W cm^{-2}, 1kHz, pulse width 35 fs) at 730 nm using a laser source equipped in an LSM 710 Carl Zeiss Laser Scanning Confocal Microscope. The whole procedure was processed in the dark. Fluorescent images were captured before and after the irradiation using an exitation wavelength at 488 nm and emission wavelength between 510 and 550 nm.

Annexin V-FITC/propidium iodide double stainning assay

Adherent HeLa cells preincubated with 0.5 μM **Ir1-Ir3** (0.5% DMSO, v%) for 30 min at 37 °C, respectively were further live stained with annexin V-FITC and propidium iodide following the protocols of the manufacturer (Life Technologies) and imaged before and 30 minutes after the TPA-PDT treatment (730 nm, 0.88 W cm^{-2}, 1kHz, pulse width 35 fs, irradiation for 50 s). For Annexin V-FITC channel, the exitation wavelength was 488 nm, and the emission filter was between 500 and 530 nm; for the PI detection, the exitation wavelength was 536 nm, and the signals were collected between 600-630 nm.

Realtime monitoring of cell morphological changes in TPA-PDT duration

Adherent HeLa cells pretreated with 0.5 μM **Ir1** (0.5% DMSO, v%) for 30 min at 37 °C were exposed to two-photon laser source for a duration of 100 seconds (0.88 W cm^{-2}, 1kHz, pulse width 35 fs). The cell morphological changes were recorded during the PDT treatment.

Formation of 3D multicellular tumor spheroids (MCTSs)[3]

A suspension of 1% agarose in DMEM was sterilized by a high pressure steam sterilizaition pot for 20 min. The resulting gel was charged into 96-well microassya culture plates (50 μL/well) before cool down. The prepared plates were then exposed under UV irradiation for 3 h to ensure totally sterile. A suspension of HeLa cells at 2 × 10^4 cells/mL was split charged into the prepared 96-well microassay culture plates with a volume of 200 μL/well. The culture medium was refreshed every two days. HeLa MCTSs formed spontaneously in 3 days with a diameter around 400 μm.

Photocytotoxicity assay

Photocytotoxicity assay was conducted to assess the photodynamic theraputic outcome of **Ir1-Ir3** complexes in both monolayer cells and 3D MCTSs. And H_2TPP was adopted as the positive control. For monolayer cell viability test, exponentially grown HeLa/L02 cells were seeded in triplicate into 96-well white-walled plates (Corning, non-transparent bottom) at 1 × 10^4 cells/well and incubated for 24 h to adhere. For 3D models, the HeLa MCTSs cultured by the afore mentioned method were carefully transferred to 96-well white-walled plates (Corning, non-transparent bottom, 1 spheroid per well). Both monolayer cells and MCTSs were treated with increasing concentration of the tested compounds. Control wells were prepared by the addition of culture medium (100 μL/well). Wells containing only culture medium, namely, without any cells, were used as the blank. All plates were incubated in the dark for 12 h. Then all of the culture medium were refreshed. For the light group of both monolayer cells and MCTSs, all of the expriment, control and blank wells were irradiated with light source in distinct manner. In detail, the monolayer cells were exposed to OPA irradiation (405 ± 10 nm, 40 mW cm^{-2}, light dose = 12 J cm^{-2}). While the MCTSs light group was equally devided into two groups, one subjected to OPA irradiation (405 ± 10 nm, 40 mW cm^{-2}, light dose = 12 J cm^{-2}), the other TPA irradiation (730 nm, 0.88 W cm^{-2}, 1kHz, pulse width 35 fs, light dose = 12 J cm^{-2}/section, section interval = 3 μm). Both of the cells from the dark and light groups were incubated for additional 36 h. Upon completion, the viability and IC_{50} values of monolayer cells and MCTSs were obtained by the ATP concentration determination with the CellTitler-Glo® Luminescent Cell Viability kit (Promega) and CellTitler-Glo® 3D Cell Viability kit (promega), respectively.[16] The luminescence were measured on an infinite M200 PRO equipment (TECAN). The cell survival rate in the control wells of the dark group was considered as the 100% cell survival. IC_{50} values

were determined by plotting the percentage of viability versus concentration on a logarithmic graph.

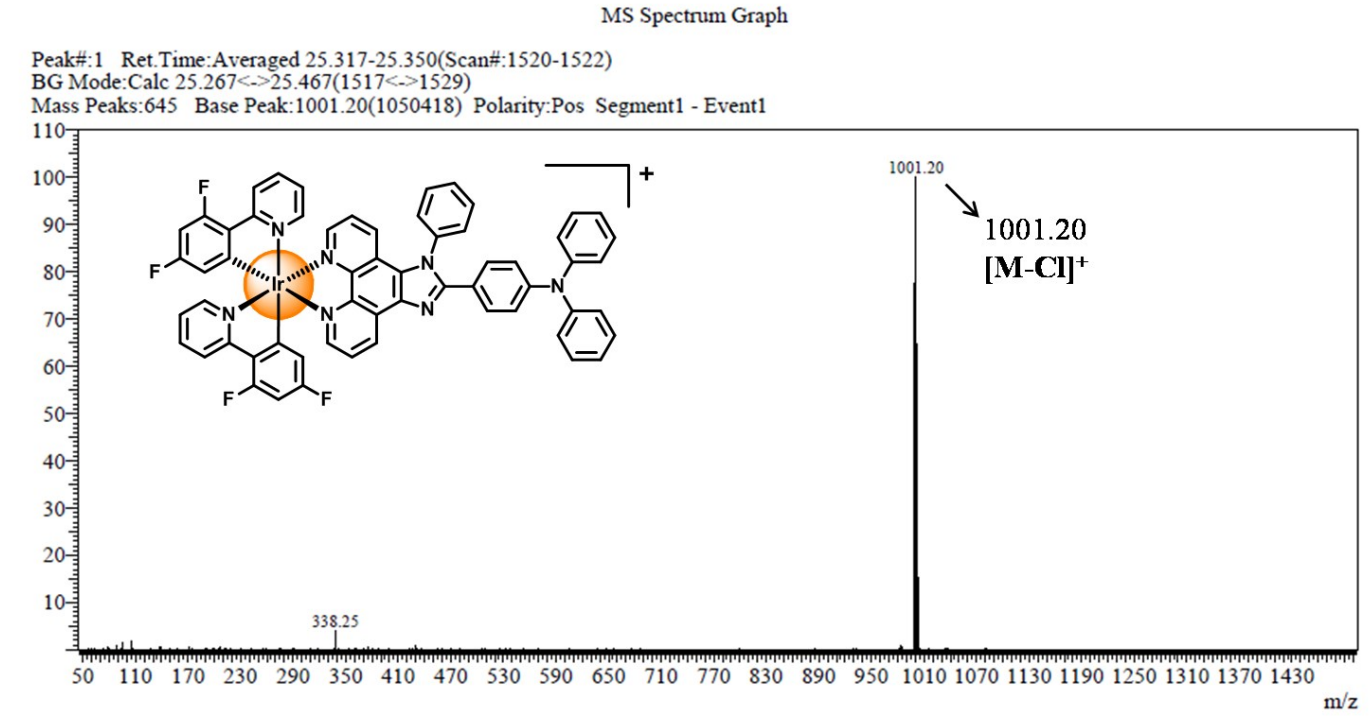
MS Spectrum Graph
Peak#:1 Ret.Time:Averaged 25.317-25.350(Scan#:1520-1522)
BG Mode:Calc 25.267<->25.467(1517<->1529)
Mass Peaks:645 Base Peak:1001.20(1050418) Polarity:Pos Segment1 - Event1
1001.20
1001.20
[M-Cl]+
338.25
m/z

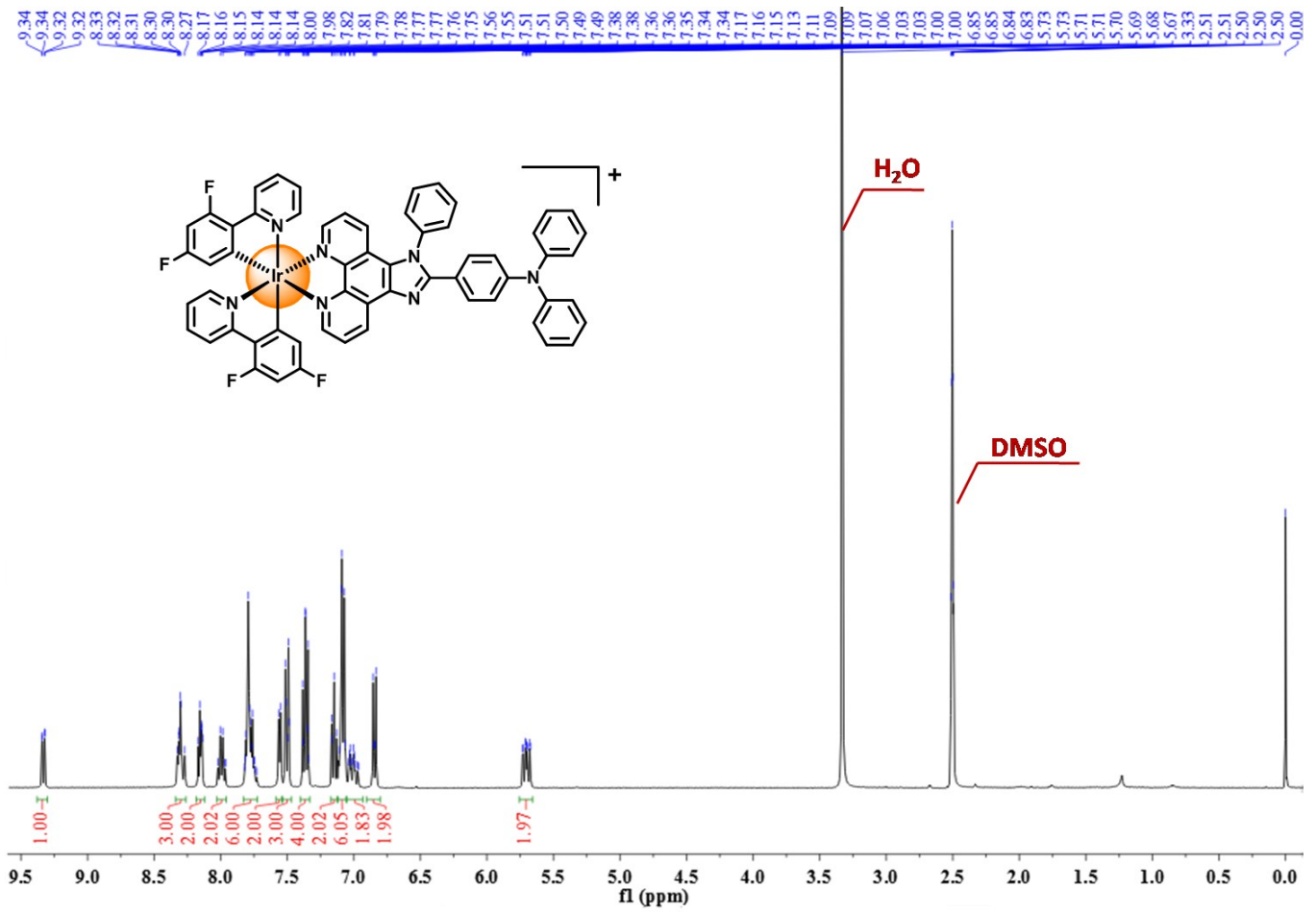
H2O
DMSO
fl (ppm)

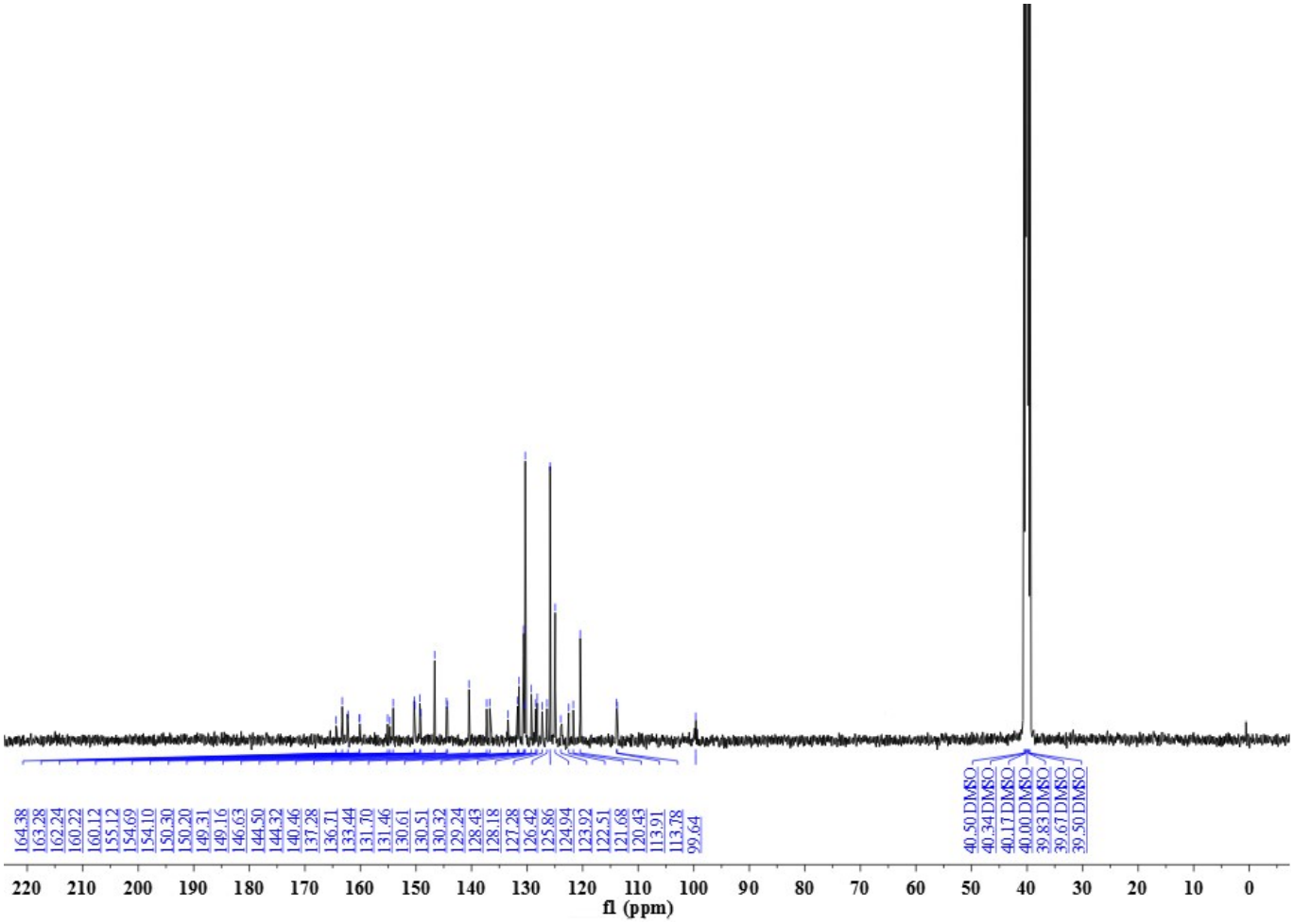

Figure S1. ESI-MS, ^{1}H NMR and ^{13}C NMR spectrum of **Ir1**。

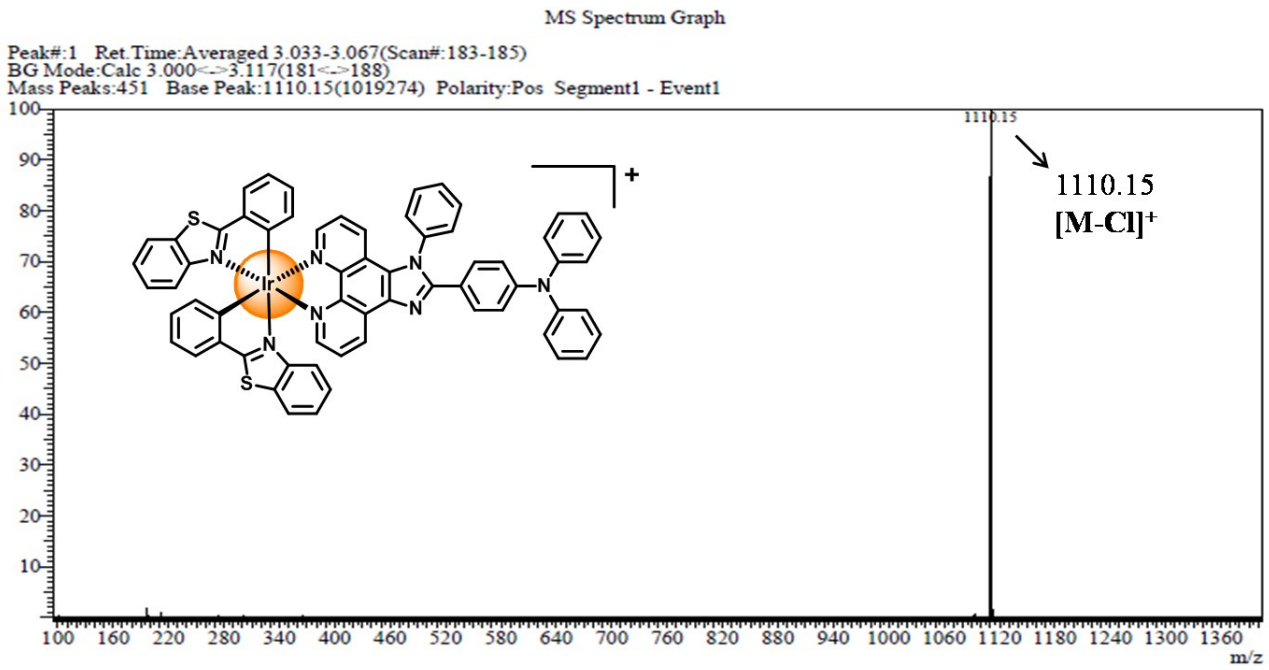
MS Spectrum Graph
Peak#:1 Ret.Time:Averaged 3.033-3.067(Scan#:183-185)
BG Mode:Calc 3.000<->3.117(181<->188)
Mass Peaks:451 Base Peak:1110.15(1019274) Polarity:Pos Segment1 - Event1
1110.15
1110.15
[M-Cl]+
m/z

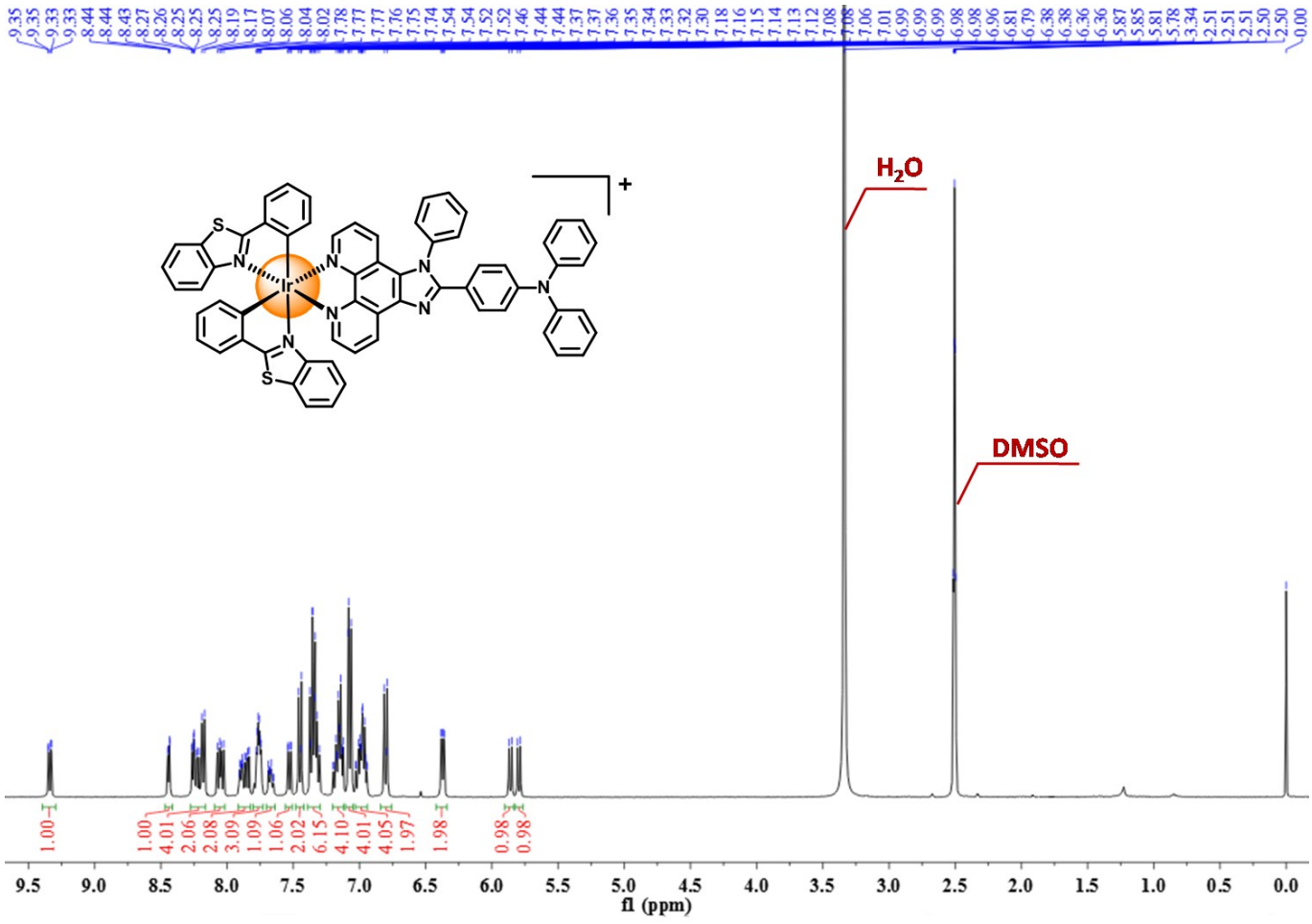
H2O
DMSO
fl (ppm)

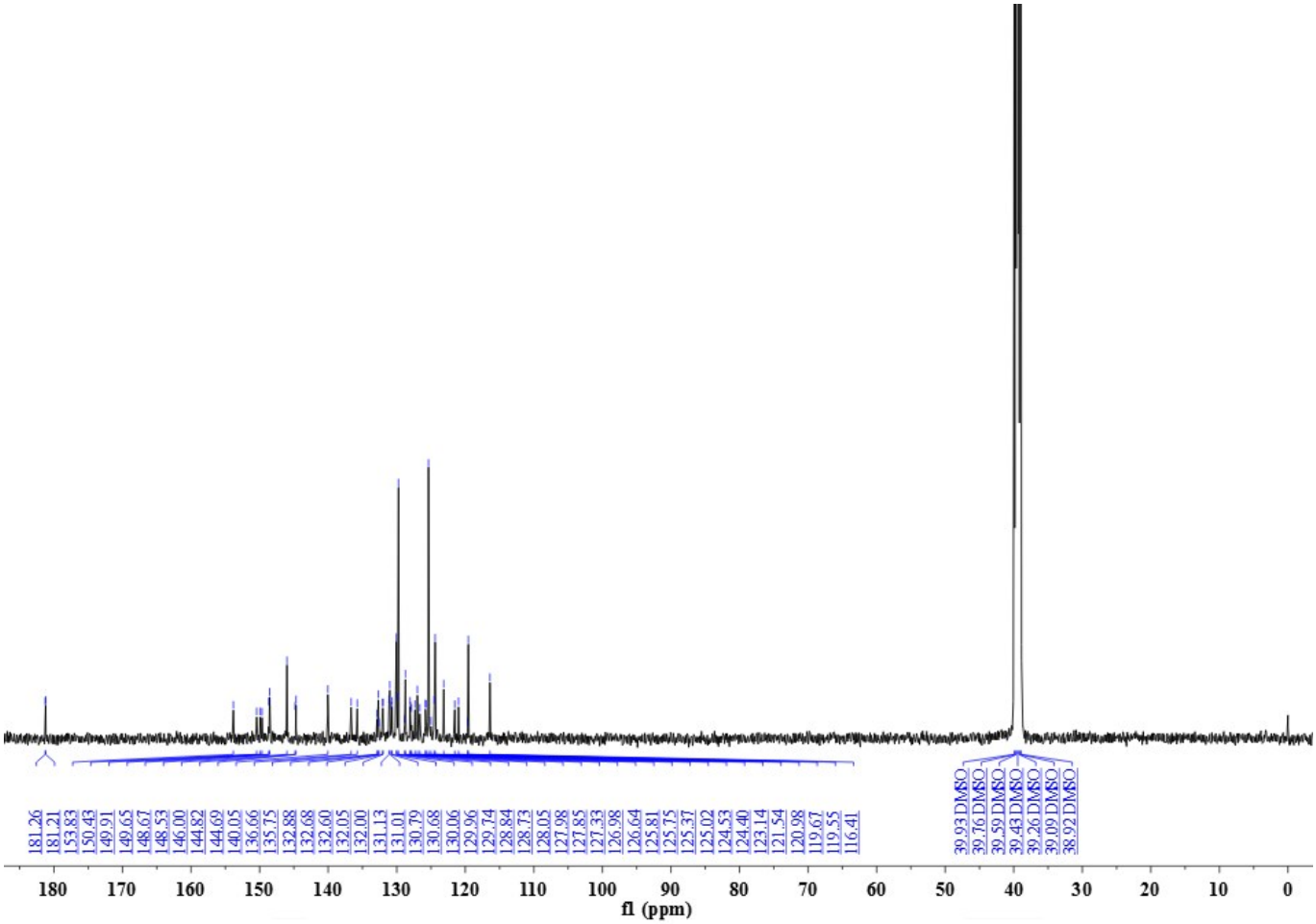

Figure S2. ESI-MS, ^{1}H NMR and ^{13}C NMR spectrum of **Ir2**。

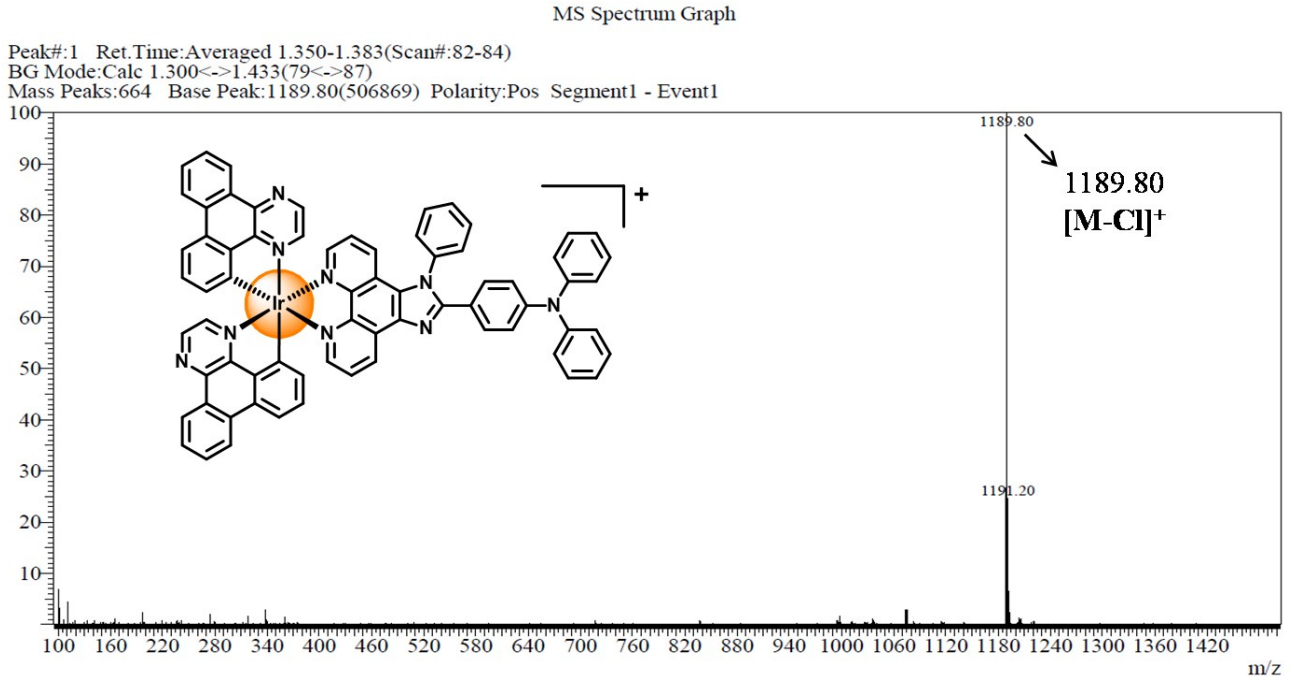
MS Spectrum Graph
Peak#:1 Ret.Time:Averaged 1.350-1.383(Scan#:82-84)
BG Mode:Calc 1.300<->1.433(79<->87)
Mass Peaks:664 Base Peak:1189.80(506869) Polarity:Pos Segment1 - Event1
1189.80
1189.80
[M-Cl]+
1191.20
m/z

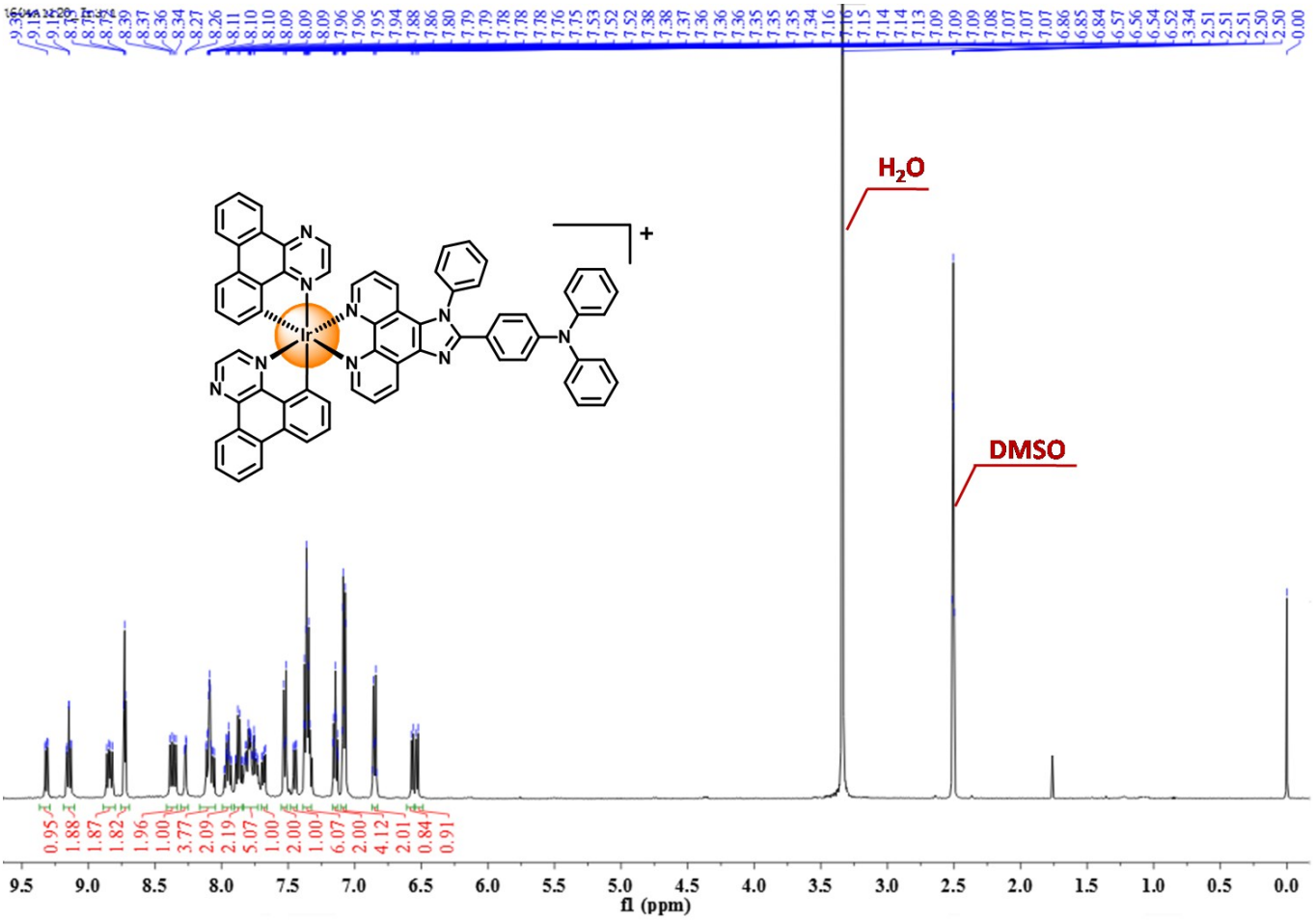
H2O
DMSO
fl (ppm)

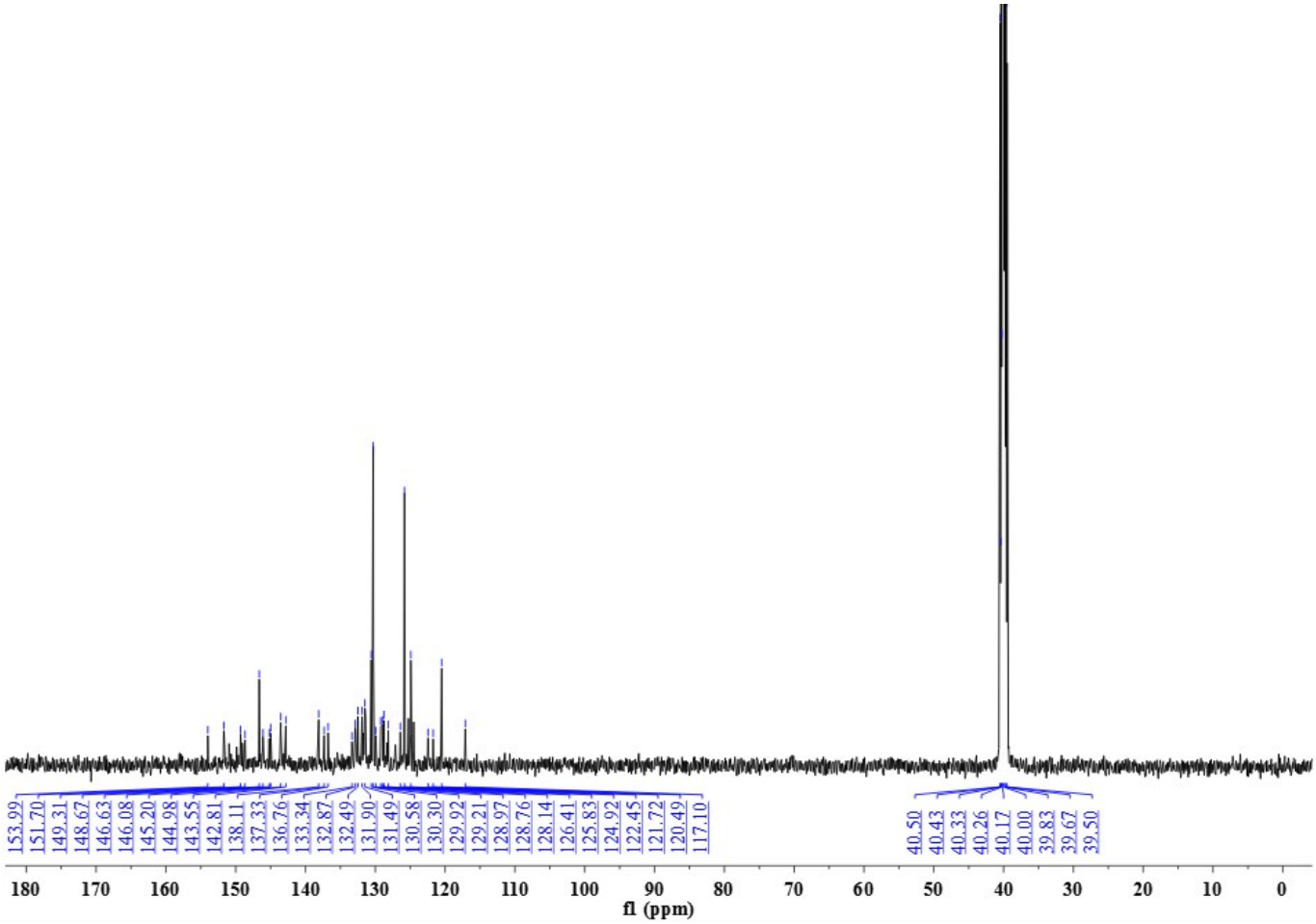

Figure S3. ESI-MS, ^{1}H NMR and ^{13}C NMR spectrum of **Ir3**。

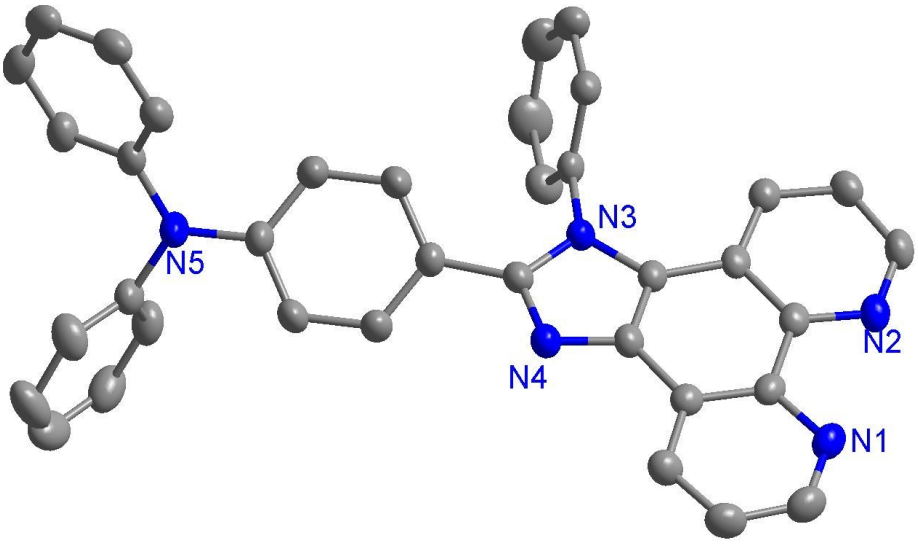

Figure S4. X-ray crystal structure of **dpipa**. The H atoms and solvent have been omitted for clarity. Only the major conformation of the disorder is shown in this figure.

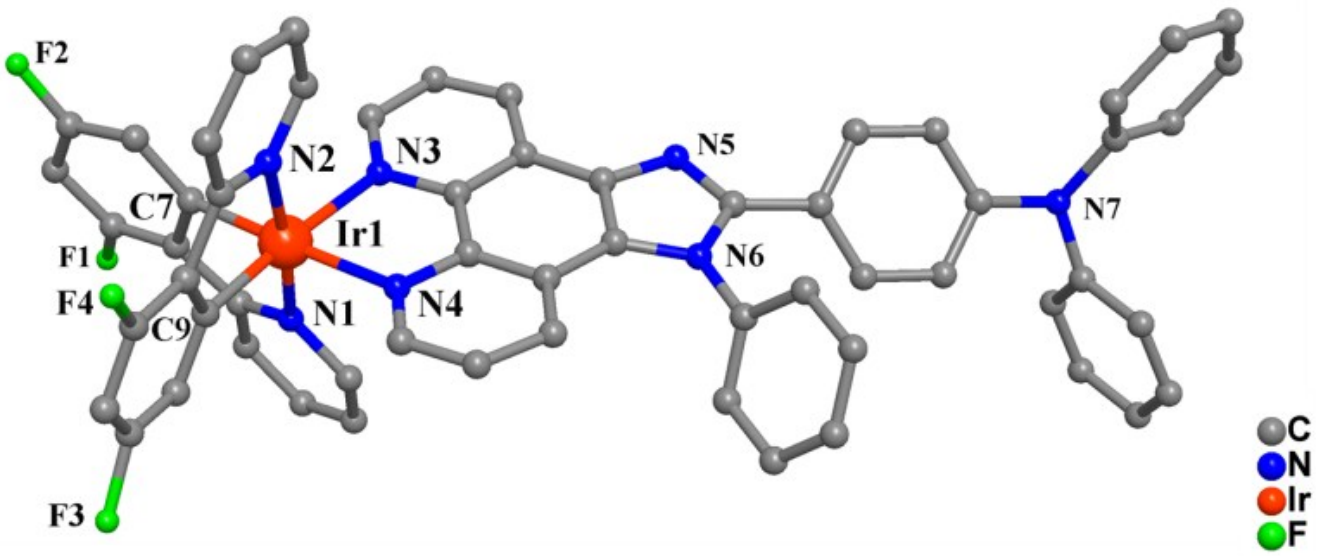

Figure S5. X-ray crystal structure of **Ir1**. The H atoms, counter anion and solvent have been omitted for clarity. Only the major conformation of the disorder is shown in this figure

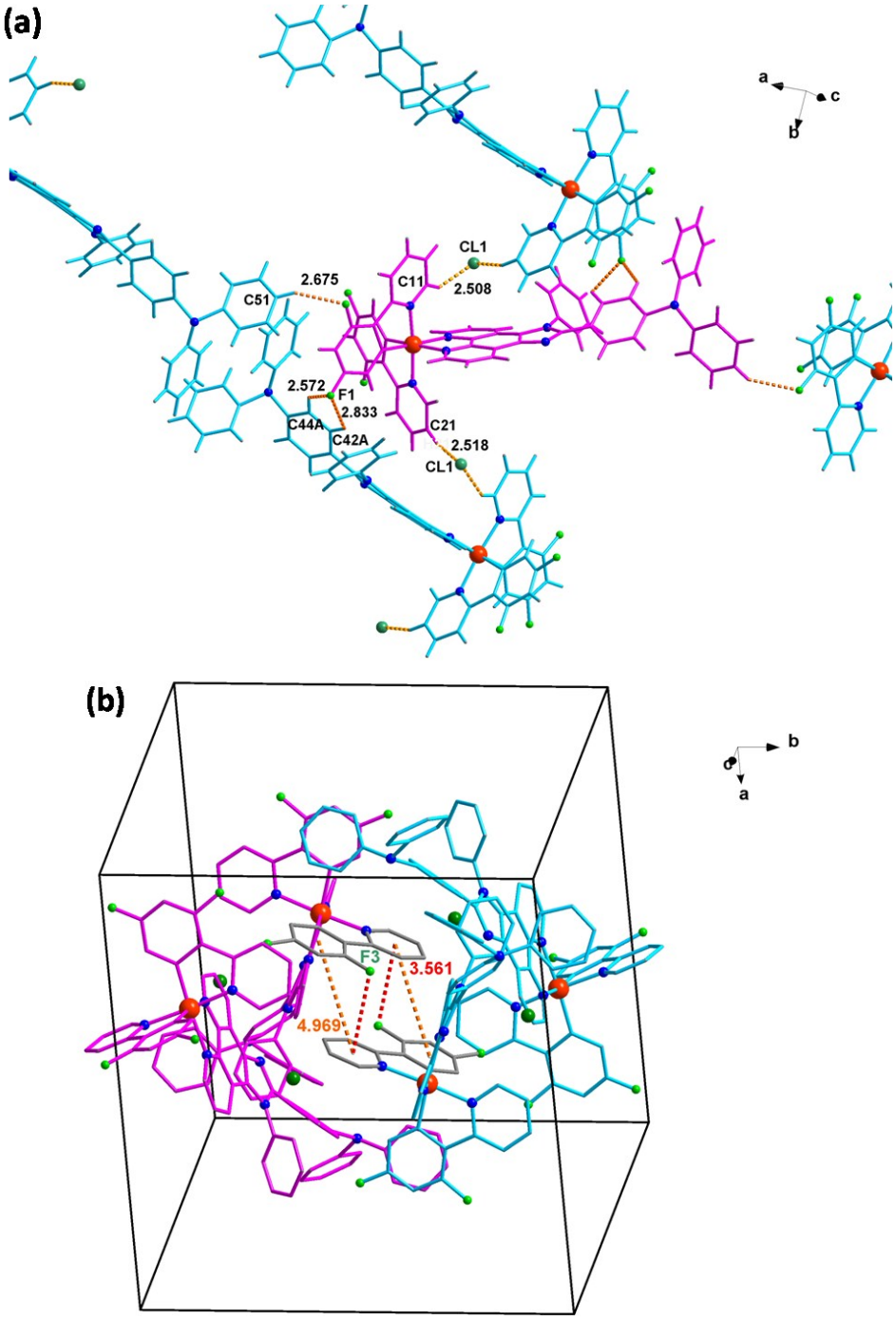

Fig. S6 The interaction diagrams in the crystal structure of **Ir1**. (a) Hydrogen bond in the crystal structure of **Ir1**. (b) C-F···π interaction between two **Ir1** molecules (Four molecules are included in a unit cell).

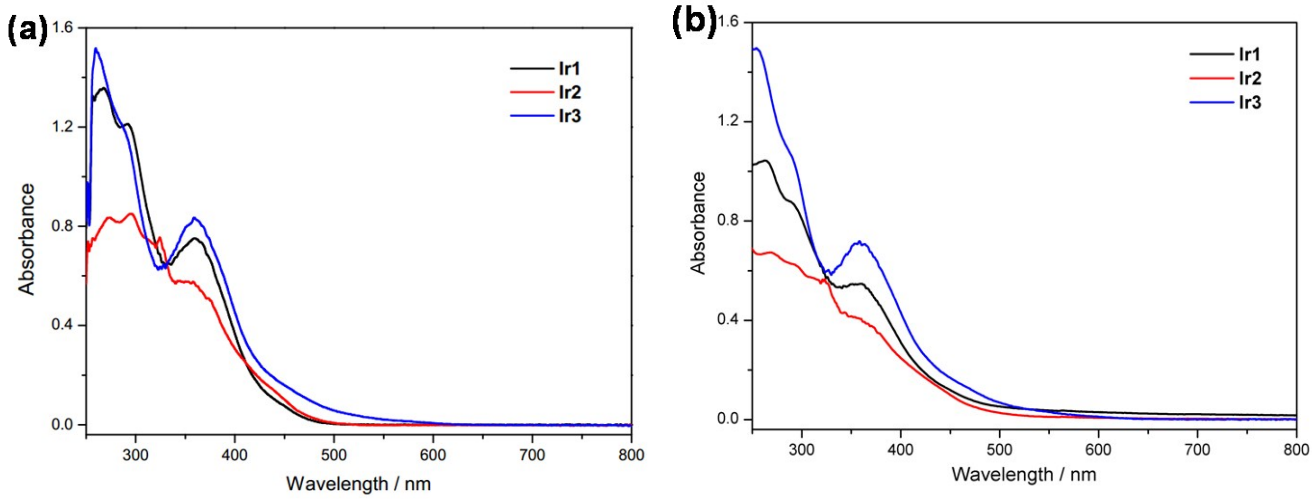

Figure S7. UV-vis absorption spectra of **Ir1-Ir3** (20 μM) in DMSO (a) and 90% water-DMSO mixtures (b).

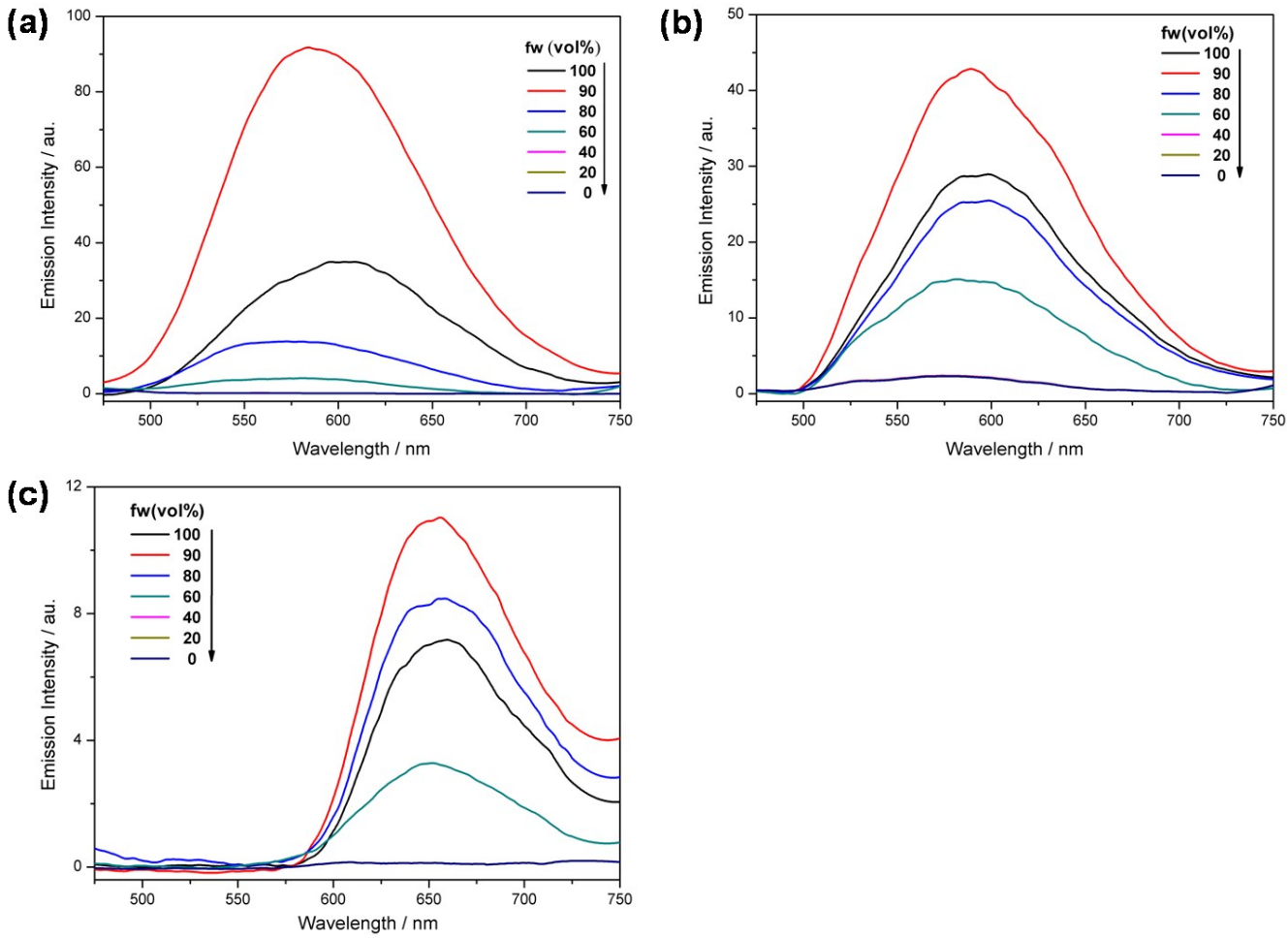

Figure S8. Fluorescence spectra of **Ir1** (a), **Ir2** (b) and **Ir3** (c), respectively, in DMSO/water mixtures with different volume fractions of water at a concentration of 20 μM. The exitation wavelength is 365 nm.

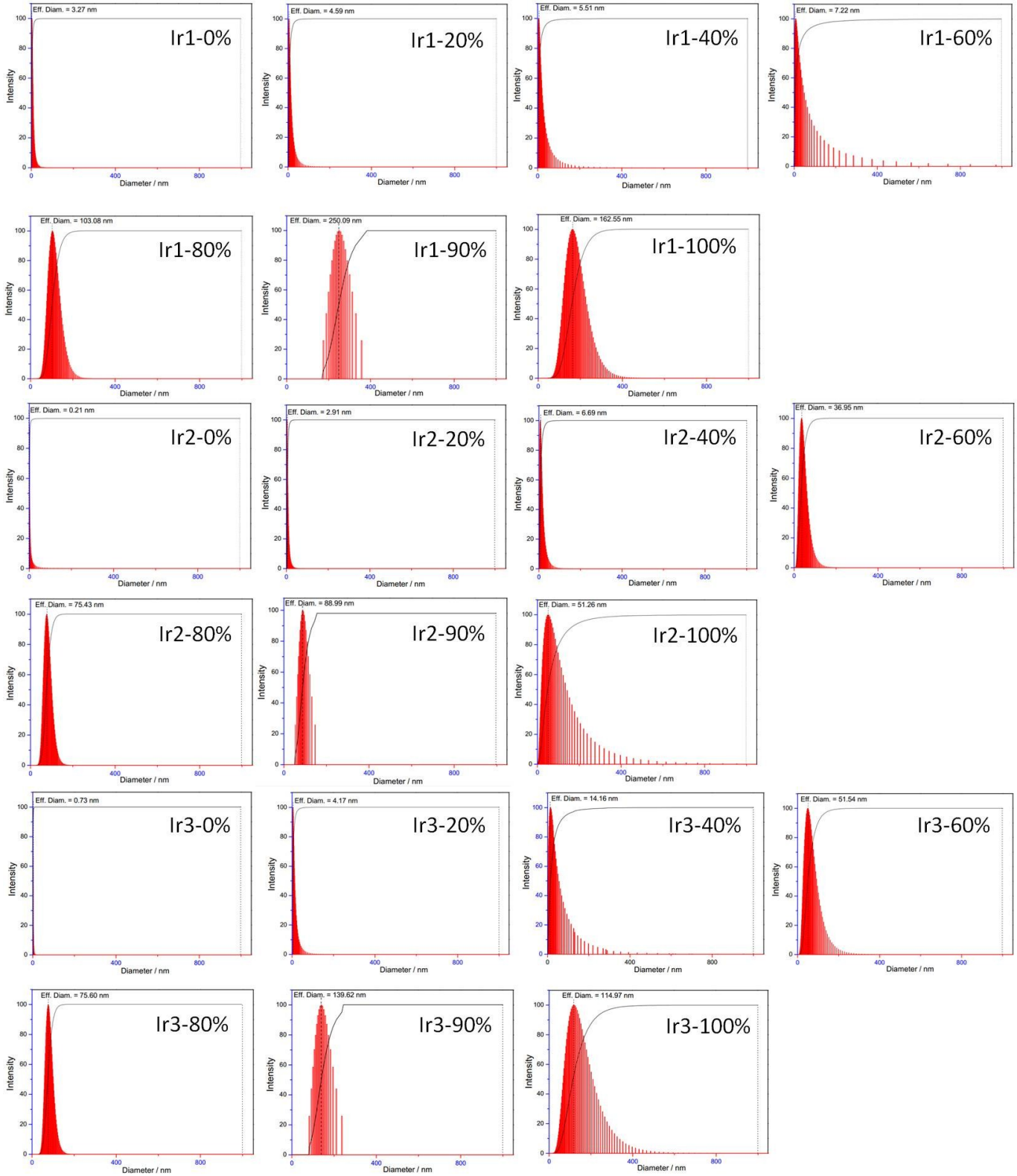

Figure S9. Hydrodynamic diameter distributions of particles of **Ir1**-**Ir3** in various ratios of water-DMSO mixture at a scattering angle of 90^{o} at 25°C (inset ratio denotes water content in the binary solvent).

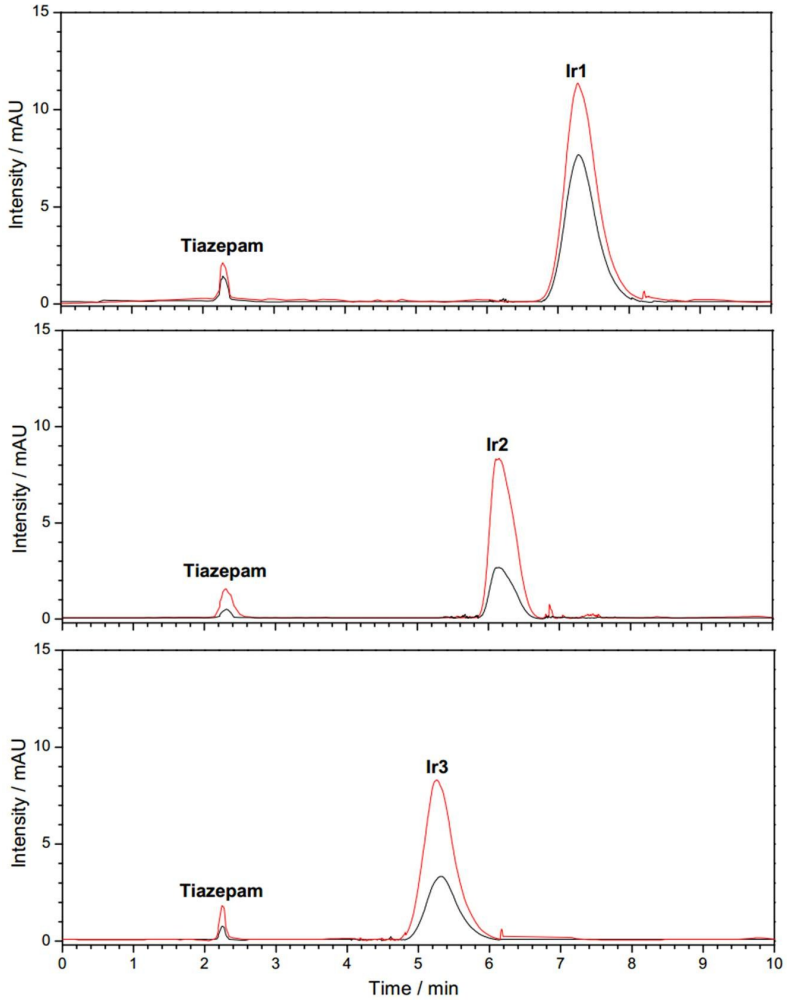

Figure S10. Stability of **Ir1-Ir3** incubated with bovine serum for 48 h (red line), the contents were tracked by HPLC-UV (Diazepam was used as internal standard), black line represents pure compounds in methanol. **Ir1** and **Ir3** were seperated with sodium pentanesulfonate (5 mM)/methanol as eluent (1:9, v/ v, 0.8 mL/min). **Ir2** was seperated with H_3PO_4 (pH 3)/methanol as eluent (1:9, v/v, 0.8 mL/min).

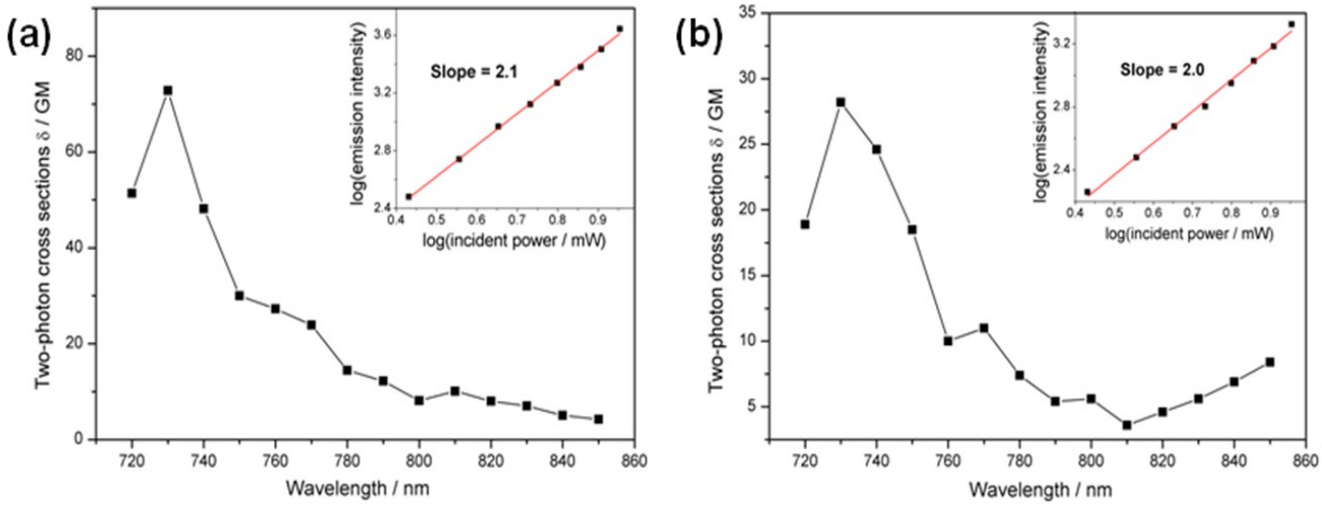

Figure S11. Two-photon cross sections of **Ir2**(a) and **Ir3**(b) versus exitation wavelength from 720 to 850 nm. Inset: the logarithmic dependence of emission intensity on incident power at 730 nm (wavelength corresponding to the maximum TPA cross
sections).

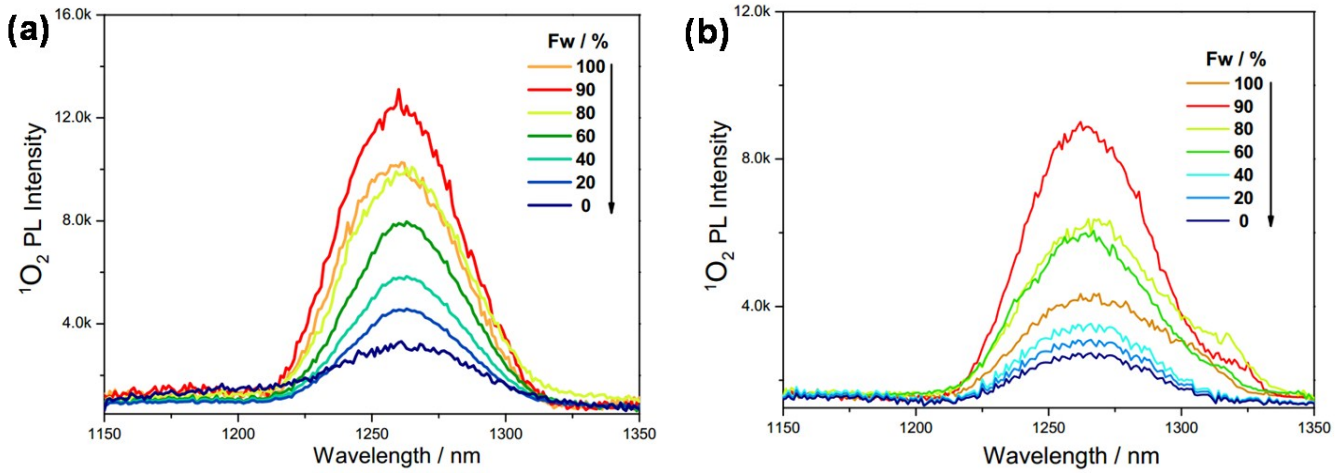

Figure S12. Singlet oxygen phosphorescence spectra in the presence of **Ir2** (a) and **Ir3** (b), respectively, in water-DMSO mixtures with different volume fractions of water at an adjusted concentration ($OD_{405\ nm}$ = 0.25). The exitation wavelength for (a) and (b) is 405 nm.

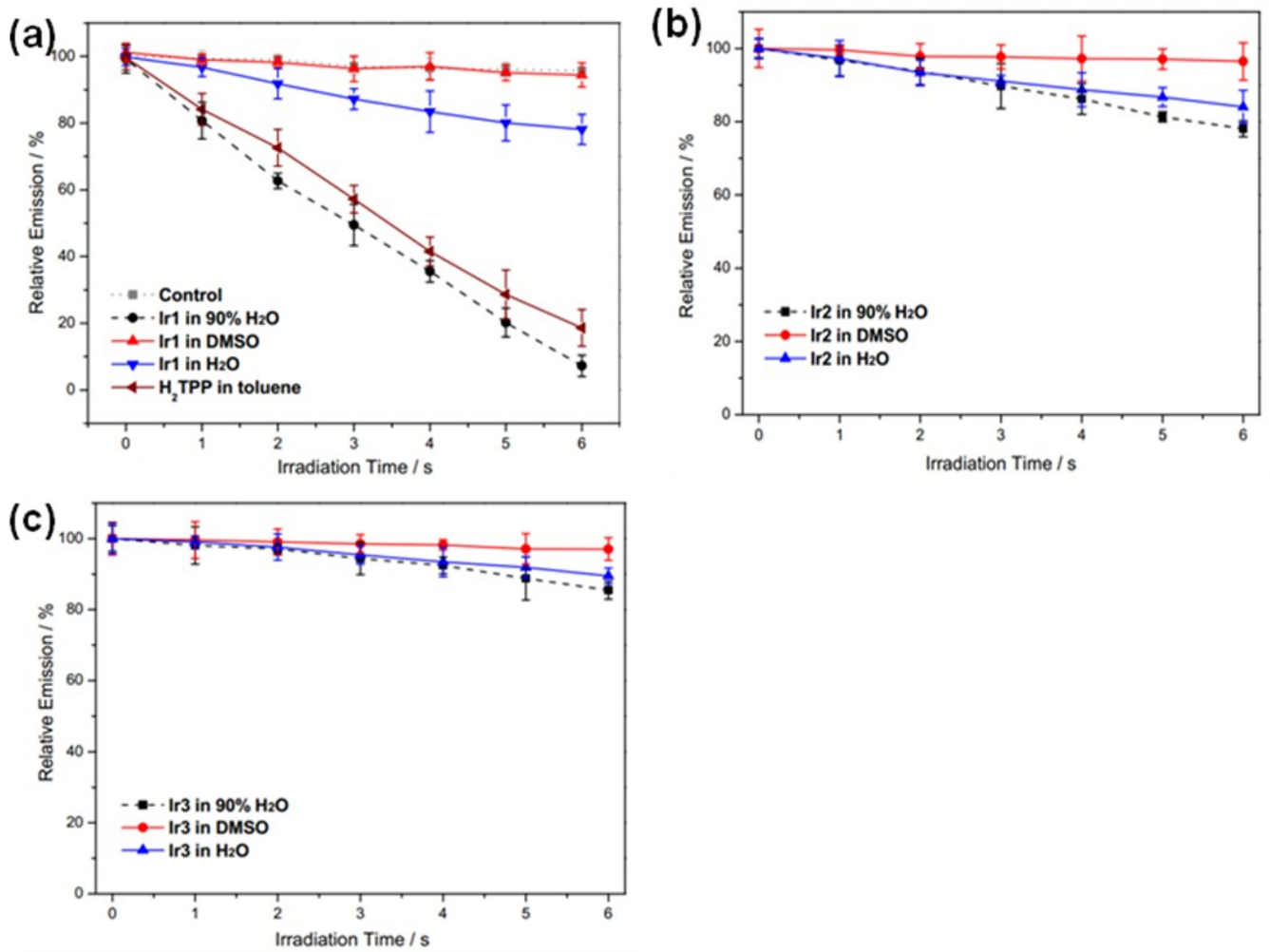

Figure S13. Plots of the relative emission change of DPBF (30 μM) at 479 nm versus irradiation time (λ_{irr}= 405 nm) in the presence of **Ir1** (a), **Ir2** (b) and **Ir3** (c), respectively, in water, DMSO or DMSO/water mixture (1:9, v/v). Plots of H_2TPP (a) in toluene were also recorded for comparison.

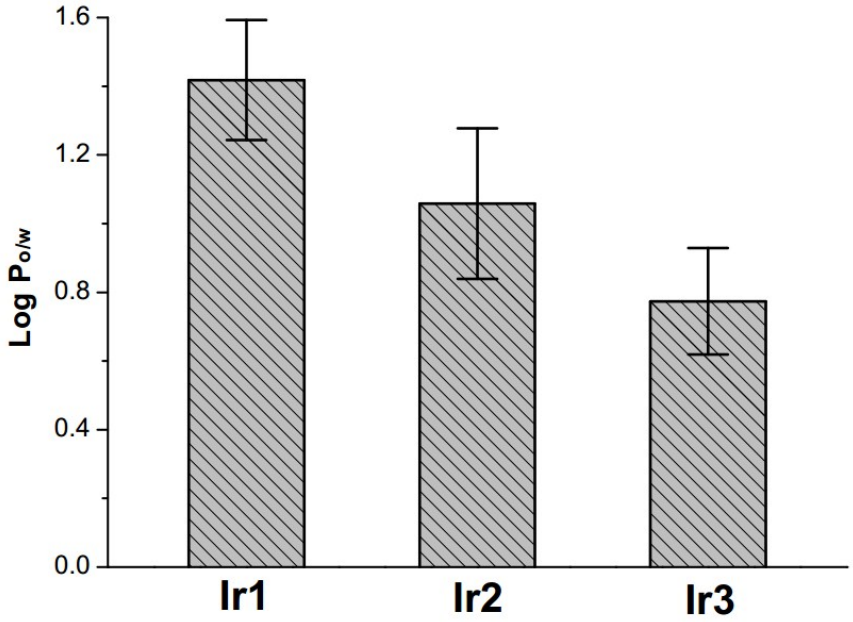

Figure S14. Octanol/water partition coefficients of **Ir1-Ir3**, the error bars denote standard deviation calculated from three replicate trials.

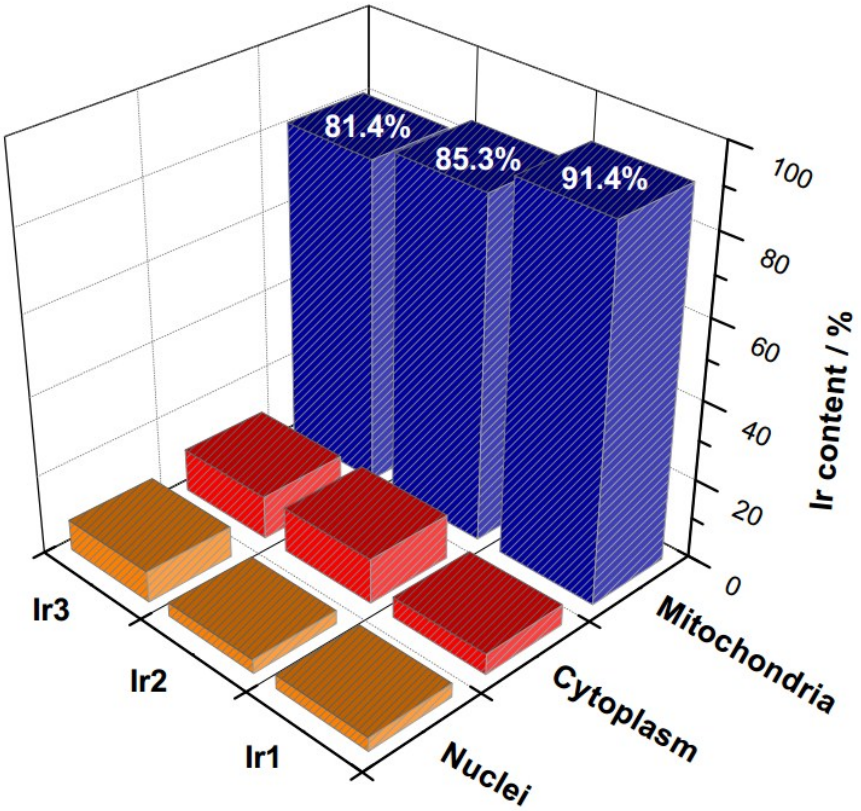

Figure S15. ICP-MS quantification of the internalized Ir by the HeLa cells. HeLa cells were treated with **Ir1-Ir3** (0.5 μM) at 37 C for 30 min in the dark. Nuclei (Nuc.), mitochondria (Mito.) and cytoplasm (without mitochondria, Cyto.) were extracted using mitochondrial and nuclear isolation kits.

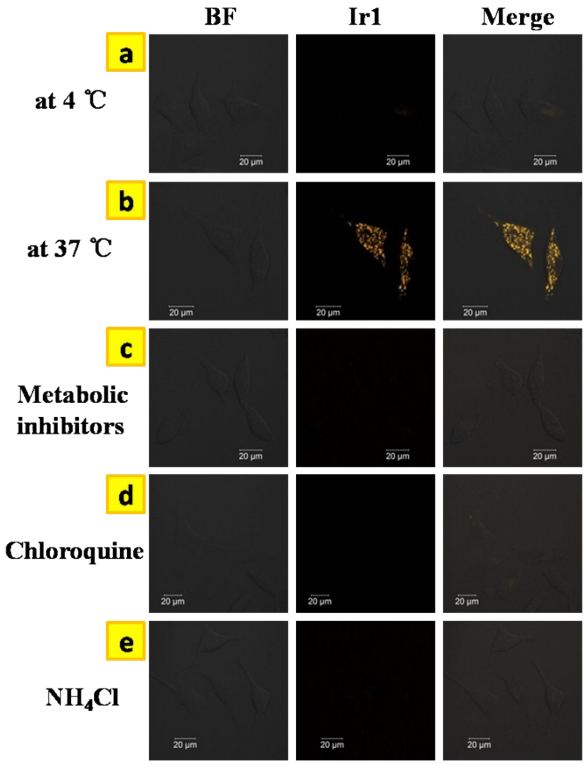

Figure S16. Confocal luminescence images and bright-field images of live HeLa cells preincubated with 0.5 μM **Ir1** for 30 min under different conditions. (a) The cells were incubated at 4 °C. (b) The cells were incubated at 37 °C. (c) The cells were incubated with 50 mM 2-deoxy-D-glucose and 5 μM oligomycin for 1 h prior to the incubation of **Ir1**. (d) The cells were treated with 50 μM Choroquine for 1 h in advance and then incubated with **Ir1**. (e) The cells were pretreated with 50 mM NH_4Cl for 1 h before the incubation of **Ir1**.

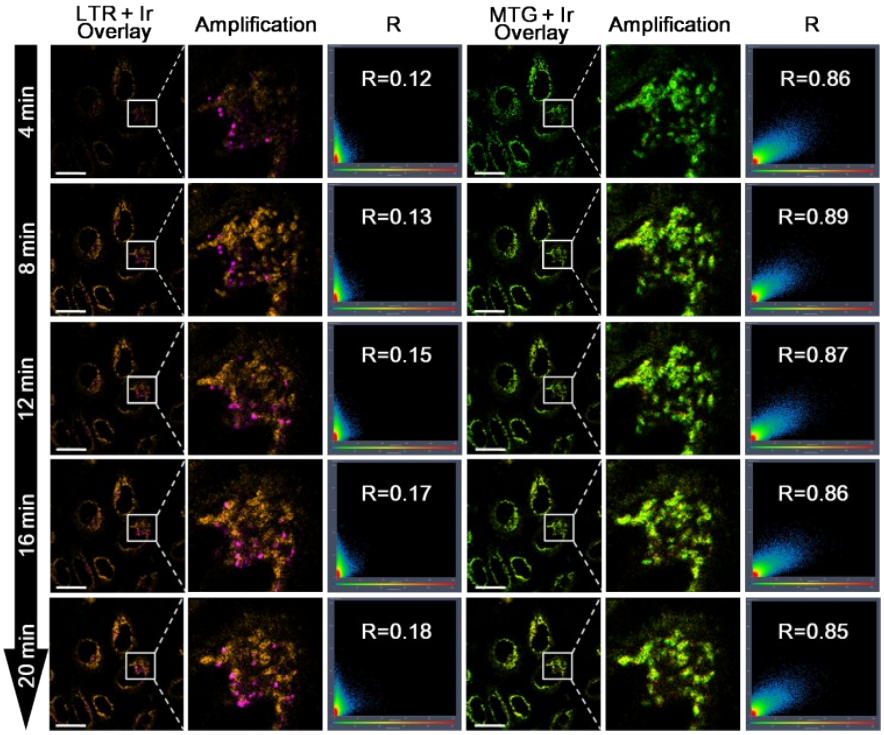

Figure S17 Co-localization of HeLa cells pre-incubated with LysoTracker Red (LTR, λ_{ex} = 543 nm, λ_{em} = 590-650 nm) and MitoTracker Green (MTG, λ_{ex} = 488 nm, λ_{em} = 505-525 nm) exposed to 0.5 μM **Ir1** (λ_{ex} = 405 nm, λ_{em} = 550-585 nm) for varying time duration. LTR channel (magenta) was processed with pseudo-colour for clarity. Inset scale bar denotes 20 μm.

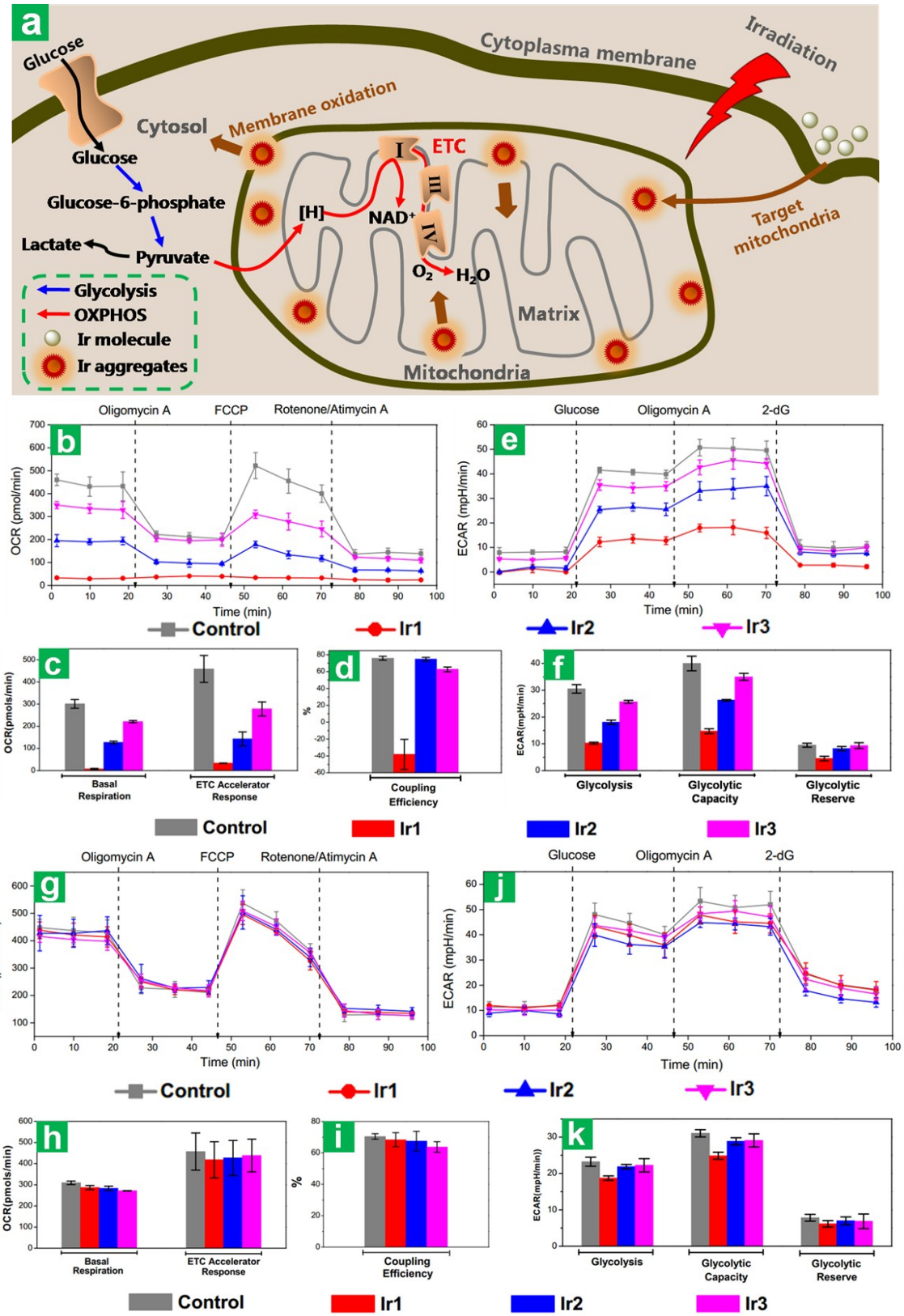

Figure S18. a) Schematic diagram of cell metabolism with mitochondria targeted Ir (0.5 μM) in PDT. b-f) Effects of **Ir1-Ir3** on HeLa cell aerobic respiration (b-d) and glycolysis (e-f) with OPA-PDT. g-k) Effects of **Ir1-Ir3** on HeLa cell aerobic respiration (g-i) and glycolysis (j-k) without OPA-PDT. OCR before the injection of oligomycin A represents the basal respiration, OCR following the injection of FCCP represents the maximal mitochondrial respiration capacity. OCR after the treatment of rotenone plus antimycin A shows the non-mitochondrial respiration. ECAR following the addition of glucose represents the glycolysis, ECAR following the injection of oligomycin A denotes the maximum glycolytic capacity, and ECAR following the addition of 2-dG shows acidification associated with non-glycolytic activity.

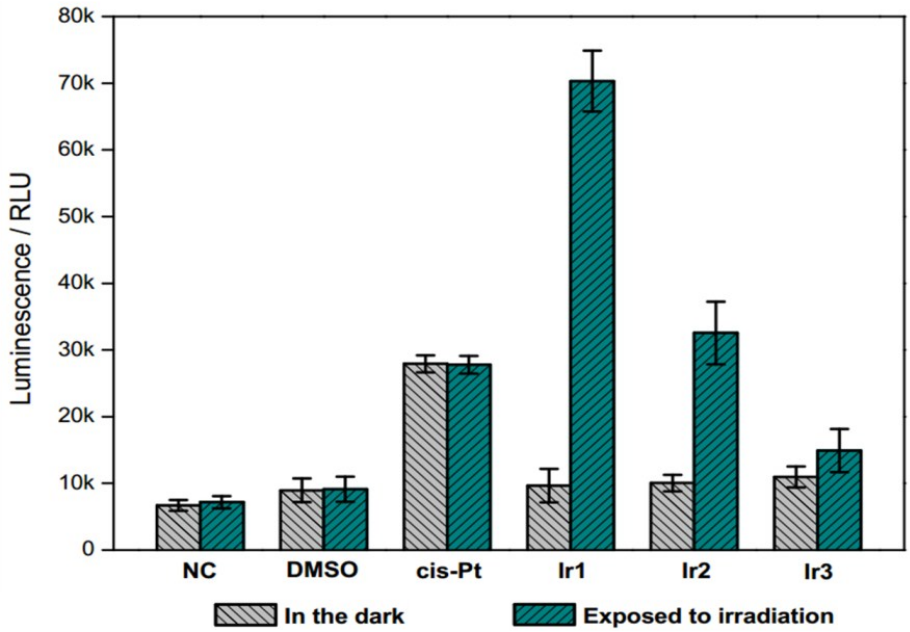

Figure S19. Activation of caspase-3/7 in HeLa cells pre-incubated with 0.5 μM **Ir1**-**Ir3** with/without OPA-PDT treatment. The measurement was conducted 2 h after the irradiation.

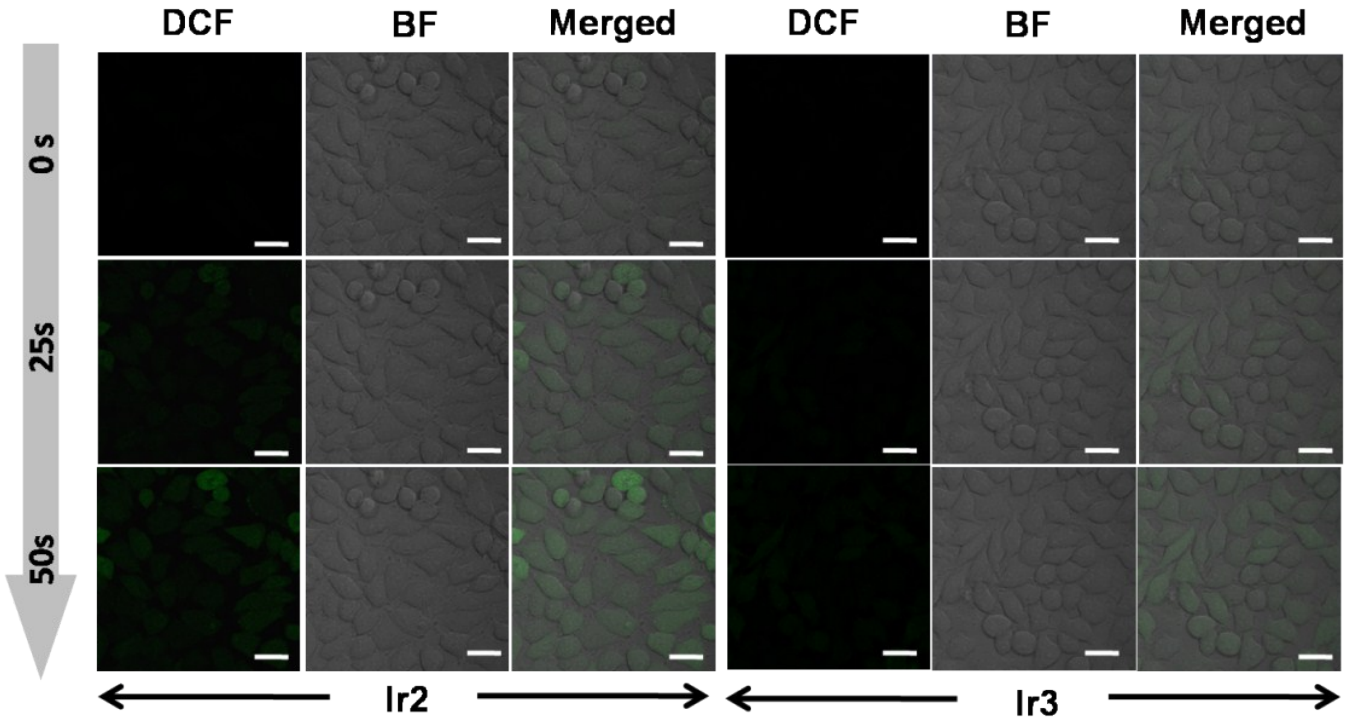

Figure S20. Confocal fluorescent images of HeLa cells incubated with DCFH-DA followed by 0.5 μM **Ir2** and **Ir3**, respectively, before and after two-photon irradiation (0.88 W cm^{-2}, 1kHz, pulse width 35 fs) at 730 nm. Inset scale bars: 20 μm.

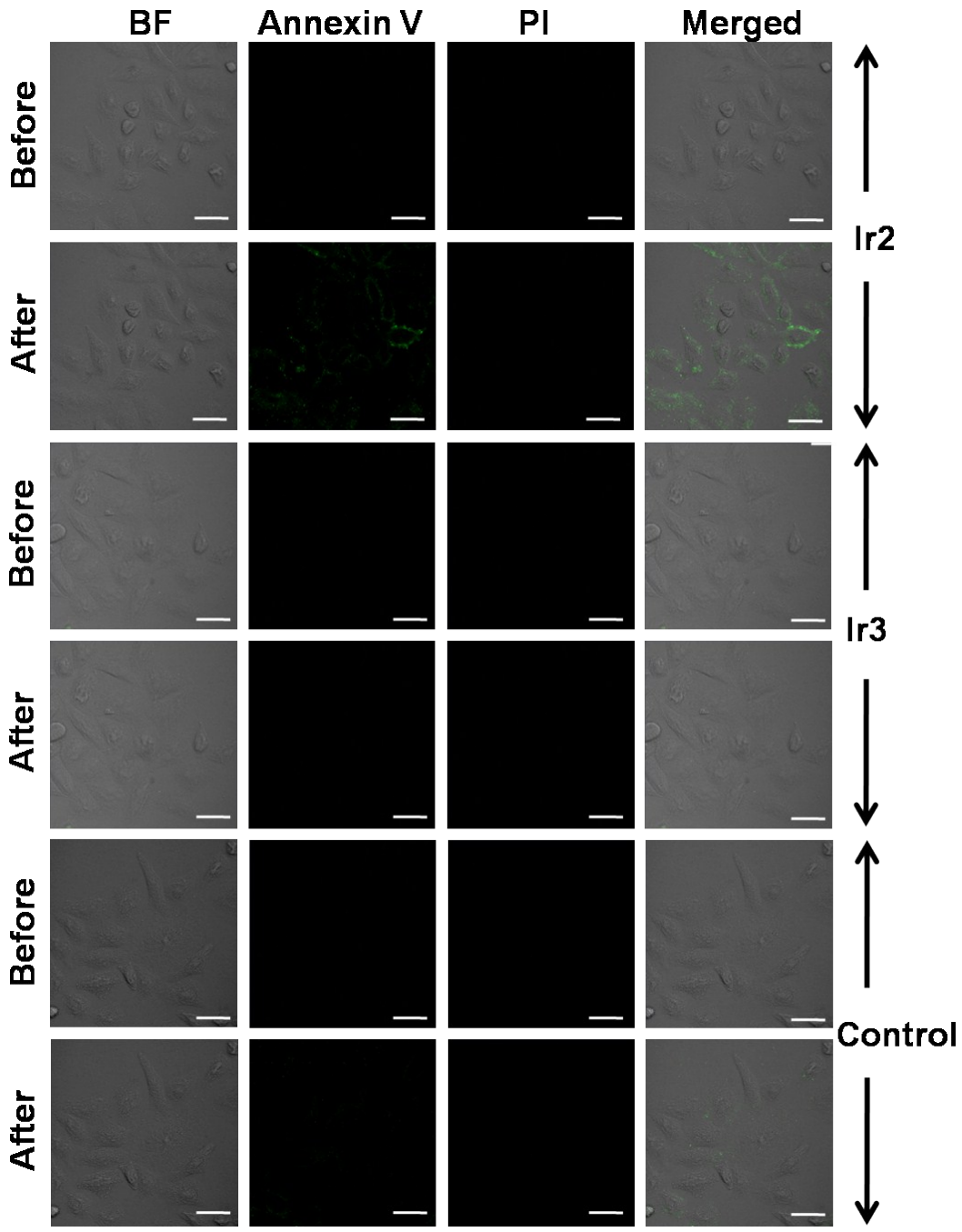

Figure S21. Confocal imaging of cell apoptosis with Annexin V-FITC/PI co-staining in HeLa cells. The cells were pretreated with culture medium (Control), 0.5 μM **Ir2** and **Ir3**, respectively and subjected to two-photon irradiation for 50 s (730 nm, 0.88 W cm^{-2}, 1kHz, pulse width 35 fs) in advance. Inset scale bars: 20 μm.

Table S1. Crystal data and structure refinement for **dpipa.**

Identification code	A
Empirical formula	$C_{37}H_{25}N_5$
Formula weight	539.62
Temperature/K	293(2)
Crystal system	monoclinic
Space group	$P2_1/c$
a/Å	13.981(2)
b/Å	9.6424(17)
c/Å	20.807(4)
α/°	90
β/°	90.981(4)
γ/°	90
Volume/Å^3	2804.5(9)
Z	4
ρ_{calc}g/cm^3	1.278
μ/mm^{-1}	0.077
F(000)	1128.0
Crystal size/mm^3	0.309 × 0.232 × 0.216
Radiation	MoKα (λ = 0.71073)
2Θ range for data collection/°	6.426 to 54.906
Index ranges	-18 ≤ h ≤ 18, -12 ≤ k ≤ 12, -26 ≤ l ≤ 26
Reflections collected	21045
Independent reflections	6369 [R_{int} = 0.0534, R_{sigma} = 0.0564]
Data/restraints/parameters	6369/0/379
Goodness-of-fit on F^2	1.017
Final R indexes [I>=2σ (I)]	R_1 = 0.0477, wR_2 = 0.1293
Final R indexes [all data]	R_1 = 0.0789, wR_2 = 0.1625
Largest diff. peak/hole / e Å^{-3}	0.32/-0.27

Table S2. Bond lengths (Å) and angles (°) for **dpipa**

Bond length (Å)	N2-C12	1.363(2)	N5-C32	1.440(2)
	N2-C10	1.334(2)	N5-C23	1.419(2)
	N4-C5	1.382(2)	C15-C14	1.386(3)
	N4-C13	1.329(2)	C15-C16	1.395(3)
	N1-C11	1.362(2)	C21-C22	1.384(3)
	N1-C1	1.330(2)	C14-C19	1.397(3)
	N3-C6	1.394(2)	C25-C24	1.388(3)
	N3-C13	1.391(2)	C22-C23	1.400(3)
	N3-C14	1.449(2)	C26-C27	1.402(3)
	C7-C6	1.444(2)	C26-C31	1.396(3)
	C7-C12	1.431(2)	C24-C23	1.400(3)
	C7-C8	1.410(2)	C32-C33	1.393(3)
	C6-C5	1.384(2)	C32-C37	1.385(3)
	C12-C11	1.473(3)	C28-C27	1.390(3)
	C5-C4	1.436(2)	C28-C29	1.385(3)
	C11-C4	1.420(2)	C33-C34	1.382(3)
	C4-C3	1.410(2)	C31-C30	1.392(3)
	C10-C9	1.400(3)	C30-C29	1.387(3)
	C13-C20	1.481(2)	C16-C17	1.387(3)
	C20-C21	1.401(2)	C18-C19	1.388(3)
	C20-C25	1.404(2)	C18-C17	1.387(3)
	C2-C3	1.377(3)	C35-C34	1.372(3)
	C2-C1	1.403(3)	C35-C36	1.384(4)
	C9-C8	1.375(2)	C37-C36	1.395(3)
	N5-C26	1.428(2)		
Bond angles (°)	C10-N2-C12	117.94(15)	C26-N5-C32	119.27(14)
	C13-N4-C5	104.86(14)	C23-N5-C26	122.52(15)
	C1-N1-C11	117.51(16)	C23-N5-C32	118.18(15)
	C6-N3-C14	127.19(14)	C14-C15-C16	119.21(18)
	C13-N3-C6	106.44(13)	C22-C21-C20	120.96(17)
	C13-N3-C14	125.91(13)	C15-C14-N3	120.24(16)
	C12-C7-C6	116.04(15)	C15-C14-C19	121.40(16)
	C8-C7-C6	126.39(15)	C19-C14-N3	118.34(16)
	C8-C7-C12	117.56(15)	C24-C25-C20	121.65(16)
	N3-C6-C7	131.58(15)	N1-C1-C2	124.33(17)
	C5-C6-N3	105.15(14)	C21-C22-C23	121.25(17)
	C5-C6-C7	123.26(15)	C27-C26-N5	120.97(17)
	N2-C12-C7	122.12(15)	C31-C26-N5	120.18(18)
	N2-C12-C11	116.86(15)	C31-C26-C27	118.83(17)
	C7-C12-C11	121.01(15)	C25-C24-C23	120.34(17)

	N4-C5-C6	111.47(15)	C33-C32-N5	119.57(17)
	N4-C5-C4	126.98(14)	C37-C32-N5	121.26(17)
	C6-C5-C4	121.51(15)	C37-C32-C33	119.15(18)
	N1-C11-C12	117.70(15)	C29-C28-C27	120.5(2)
	N1-C11-C4	121.99(15)	C28-C27-C26	120.37(18)
	C4-C11-C12	120.30(14)	C34-C33-C32	120.25(19)
	C4-C11-C5	117.87(14)	C30-C31-C26	120.1(2)
	C3-C4-C5	123.48(15)	C31-C30-C29	120.77(2)
	C3-C4-C11	118.65(15)	C17-C16-C15	119.71(19)
	N2-C10-C9	123.84(16)	C22-C23-N5	121.98(16)
	N4-C13-N3	112.07(14)	C24-C23-N5	119.75(16)
	N4-C13-C20	122.00(15)	C24-C23-C22	118.24(16)
	N3-C13-C20	125.83(14)	C19-C18-C17	120.3(2)
	C21-C20-C13	125.36(16)	C28-C29-C30	119.39(19)
	C21-C20-C25	117.55(16)	C34-C35-C36	119.4(2)
	C25-C20-C13	117.09(15)	C18-C19-C14	118.7(2)
	C3-C2-C1	118.86(17)	C35-C34-C33	120.8(2)
	C8-C9-C10	118.92(16)	C32-C37-C36	119.9(2)
	C9-C8-C7	119.61(16)	C16-C17-C18	120.63(2)
	C2-C3-C4	118.63(17)	C35-C36-C37	120.4(2)

Table S3. Crystal data and structure refinement for **Ir1.**

Identification code	1
Empirical formula	$C_{59}H_{37}ClF_4IrN_7$
Formula weight	1147.60
Temperature/K	293(2)
Crystal system	monoclinic
Space group	$P2_1/c$
a/Å	20.8286(9)
b/Å	18.6390(6)
c/Å	17.8263(6)
α/°	90
β/°	91.188(4)
γ/°	90
Volume/Å^3	6919.1(4)
Z	4
ρ_{calc}g/cm^3	1.102
μ/mm^{-1}	4.461
F(000)	2280.0
Crystal size/mm^3	0.20 × 0.15 × 0.08
Radiation	CuKα (λ = 1.54184)
2Θ range for data collection/°	4.244 to 145.126
Index ranges	$-22 \le h \le 25$, $-18 \le k \le 22$, $-21 \le l \le 21$
Reflections collected	32146
Independent reflections	13180 [R_{int} = 0.0677, R_{sigma} = 0.0678]
Data/restraints/parameters	13180/1381/616
Goodness-of-fit on F^2	1.054
Final R indexes [I>=2σ (I)]	R_1 = 0.0745, wR_2 = 0.2021
Final R indexes [all data]	R_1 = 0.1090, wR_2 = 0.2291
Largest diff. peak/hole / e Å^{-3}	2.54/-0.76

Table S4. Selected bond lengths (Å) and angles (°) for complex **Ir1**

Bond length (Å)	Ir1-N1	2.054(5)
	Ir1-N2	2.067(7)
	Ir1-N3	2.140(6)
	Ir1-N4	2.154(7)
	Ir1-C1	2.003(7)
	Ir1-C12	2.032(5)
Bond angles (°)	N1-Ir1-N2	175.0(2)
	N1-Ir1-N3	87.3(3)
	N1-Ir1-N4	96.6(2)
	N2-Ir1-N3	96.5(3)
	N2-Ir1-N4	87.4(3)
	N3-Ir1-N4	77.7(2)
	C1-Ir1-N1	80.1(3)
	C1-Ir1-N2	96.1(3)
	C1-Ir1-N3	98.0(3)
	C1-Ir1-N4	174.8(3)
	C1-Ir1-C1	90.2(4)
	C12-Ir1-N1	96.7(3)
	C12-Ir1-N2	79.9(3)
	C12-Ir1-N3	171.4(3)
	C12-Ir1-N4	94.2(3)

Table S5. Photophysical properties of **Ir1-Ir3**

Comd	λ_{abs}/ nm (log ε) [a]	λ_{em} / nm[b]	Φ'_{PL} [a]	Φ_{PL}[b]	σ_2[b,c]/GM	$\Phi_{PL} \times \sigma_2$[d]
Ir1	266(4.83), 359 (4.57)	584	0.001	0.044	214	9.4
Ir2	272(4.62), 349 (4.46)	589	0.006	0.021	72.8	1.5
Ir3	259(4.88), 358 (4.62)	656	0.004	0.015	28.2	0.42

[a] Data were obtained in aerated DMSO, and the exitation wavelength is 365 nm. [b] Data were obtained in aerated 90% water-DMSO mixture, and the exitation wavelength is 365 nm. [c] Maximum two-photon absorption cross section, σ_2, at 730 nm. [d] $\Phi_{PL} \times \sigma_2$ higher than the 0.1 GM threshold[17] for optical imaging application in live specimens.

Table S6. Estimation of TPA-induced ROS generating ability.[a]

Compounds	σ_2/GM	|*Slope*|[b]	|*slope*| × σ_2/ 10^2
H_2TPP	2.2[c]	13.8	0.304
Ir1	214	15.1	32.31
Ir2	72.8	3.72	2.71
Ir3	28.2	2.38	0.671

[a] Data of **Ir1-Ir3** were collected in 90% water-DMSO mixture, data of H_2TPP were measured in toluene. [b] The slopes were calculated from the linear regression of Figure S11. [c] Value taken from reference [18]

.

Table S7. The content of Ir in 10^6 HeLa cells and their distribution in nuclei, cytoplasm and mitochondria. The content of Ir in untreated cells has been subtracte.

Compd	Ir content (ng)			
	whole cell	Mitochondria	Nuclei	Cytoplasm (Without mitochondria)
Ir1	2.68 ± 0.25	2.45 ± 0.19	0.0923 ± 0. 0085	0.138 ± 0.010
Ir2	2.24 ± 0.15	1.91 ± 0.13	0.0762 ± 0. 0053	0.254 ± 0.016
Ir3	2.48 ± 0.24	2.02 ± 0.26	0.193 ± 0.015	0.268 ± 0.028

Table S8. (Photo)cytotoxicity (IC50 [μM]) towards HeLa and L02 monolayer cells.

Compound	HeLa			L02		
	Dark	OPA[a]	PI[b]	Dark	OPA[a]	PI
Cisplatin	18.2 ± 0.8	18.8 ± 0.8	0.96	17.8 ± 1.3	17.6 ± 1.9	1.0
H2TPP	> 100 [c]	30.3 ± 2.8	> 3.3	> 100	28.5 ± 1.4	> 3.5
Ir1	30.3 ± 1.2	0.40 ± 0.06	75	34.0 ± 1.7	2. 4 ± 0.2	14
Ir2	28.8 ± 2.5	2.8 ± 0.5	10	32.2 ± 0.8	4.9 ± 0.7	6.5
Ir3	29.2 ± 0.9	4.5 ± 1.1	6.5	33.8 ± 1.3	7.5 ± 1.0	4.5

[a] Irradiated at 405 nm by an LED area light (405 ± 10 nm, 40 mW cm-2, light dose = 12 J cm^{-2}). [b] PI (refers to photocytotoxicity index) is the ratio of dark-to-light toxicity and reflects the effective PDT range of the PSs. Data shown are values from three replicates. [c] The concentration cannot be higher due to its poor solubility.

Table S9. (Photo)cytotoxicity (IC_{50} [μM]) towards 400 μm 3D HeLa MCTSs.

Compound	Dark	OPA[a]	PI	TPA[b]	PI
Cisplatin	28.8 ± 2.3	27.6 ± 1.9	1.0	30.2 ± 1.7	0.95
H_2TPP	> 100	95.1 ± 3.9	nd	> 100	nd
Ir1	38.6 ± 1.7	0.82 ± 0.11	47	0.35 ± 0.5	110
Ir2	36.2 ± 2.8	6.0 ± 0.7	6.0	5.8 ± 0.9	6.2
Ir3	38.0 ± 1.3	9.5 ± 1.0	4.0	18.6 ± 1.8	2.0

[a] Irradiated at 405 nm by an LED area light (405 ± 10 nm, 40 mW cm^{-2}, light dose = 12 J cm^{-2}). [b] Irradiated at 730 nm using a confocal microscope equipped with a mode-locked Ti:sapphire laser source (0.88 W cm^{-2}, 1kHz, pulse width 35 fs light dose = 12 J cm^{-2}/section, section interval = 3 μm, scanned area for each section was *ca.* 1.5 × 1.5 mm). Data shown are values from three replicates

Reference

1 H. Ishida, S. Tobita, Y. Hasegawa, R. Katoh, K. Nozaki, *Coord. Chem. Rev*., 2010, **254**, 2449-2458.

2 (a) G. Li, Q. Lin, L. Sun, C. Feng, P. Zhang, B. Yu, Y. Chen, Y. Wen, H. Wang, L. Ji, H. Chao, *Biomaterials* **2015**, *53*, 285-295; b) J. M. G. Cowie, P. M. Toporowski, *Can. J. Chem*., 1961, **39**, 2240-2243.

3 J. Liu, Y. Chen, G. Li, P. Zhang, C. Jin, L. Zeng, L. Ji, H. Chao, *Biomaterials,* 2015, **56**, 140-153.

4 A. Kapturkiewicz, J. Nowacki, P. Borowicz, *Electro. Acta*., 2005, **50**, 3395-3400.

5 G. Li, Q. Lin, L. Ji, H. Chao, *J. Mater. Chem. B,* 2014, **2**, 7918-7926.

6 C. Jin, J. Liu, Y. Chen, R. Guan, C. Ouyang, Y. Zhu, L. Ji, H. Chao, *Sci. Rep*., 2016, **6**, 22039.

7 R. H. Blessing, *Acta Crystallogr. Sect. A: Found. Crystallogr.,* 1995, **51**, 33-38.

8 (a) O. V. Dolomanov, L. J. Bourhis, R. J. Gildea, J. A. Howard, H. Puschmann, *J. Appl. Crystallogr.,* 2009, **42**, 339-341; (b) G. M. Sheldrick, *Acta Crystallogr. Sect. A: Found. Crystallogr.,* 2008, **64**, 112-122.

9 A. L. Spek, *Acta Crystallogr.Sect. D: Bio. Crystallogr.,* 2009, **65**, 148-155.

10 W. Adam, D. V. Kazakov, V. P. Kazakov, *Chem. Revs*., 2005, **105**, 3371-3387.

11 J. Geng, C. C. Goh, W. Qin, R. Liu, N. Tomczak, L. G. Ng, B. Z. Tang, B. Liu, *Chem. Commun*. 2015, **51**, 13416-13419.

12 C. Xu, W. W. Webb, *J. Opt. Soc. Am. B,* 1996, **13**, 481-491.

13 J. Comer, K. Tam, *Helv Chim. Acta*, 1996, **79**, 1222-1238.

14 C. Li, M. Yu, Y. Sun, Y. Wu, C. Huang, F. Li, *J. Am. Chem. Soc*., 2011, **133**, 11231-11239.

15 C. Fowley, N. Nomikou, A. P. McHale, P. A. McCarron, B. McCaughan, J. F. Callan, *J. Mater. Chem*., 2012, **22**, 6456-6462.

16 H. Huang, P. Zhang, B. Yu, Y. Chen, J. Wang, L. Ji, H. Chao, *J. Med. Chem.,* 2014, dx.doi.org/10.1021/jm501095r.

17 S. S.-H. W. Toshiaki Furuta, Jami L. Dantzker, Timothy M. Dore, Wendy J. Bybee, Edward M. Callaway, Winfried Denk, Roger Y. Tsien, *Proc. Natl. Acd. Sci. USA,* 1999, **96**, 1193.

18 T. Ishi-i, Y. Taguri, S.-i. Kato, M. Shigeiwa, H. Gorohmaru, S. Maeda, S. Mataka, *J. Mater. Chem*., 2007, **17**, 3341-3346.